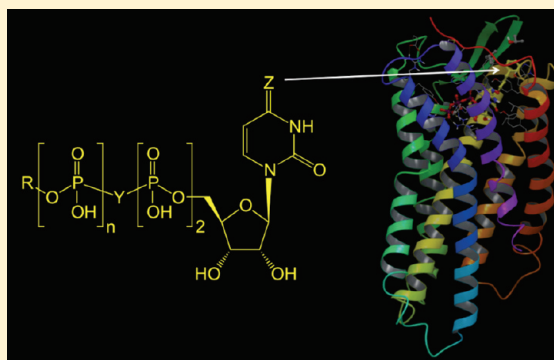


Pyrimidine Nucleotides with 4-Alkyloxyimino and Terminal Tetraphosphate  $\delta$ -Ester Modifications as Selective Agonists of the P2Y<sub>4</sub> ReceptorHiroshi Maruoka,<sup>†</sup> M. P. Suresh Jayasekara,<sup>†</sup> Matthew O. Barrett,<sup>‡</sup> Derek A. Franklin,<sup>‡</sup> Sonia de Castro,<sup>†</sup> Nathaniel Kim,<sup>†</sup> Stefano Costanzi,<sup>§</sup> T. Kendall Harden,<sup>‡</sup> and Kenneth A. Jacobson<sup>\*,†</sup><sup>†</sup>Molecular Recognition Section, Laboratory of Bioorganic Chemistry, NIDDK, National Institutes of Health, Bethesda, Maryland 20892-0810, United States<sup>‡</sup>Department of Pharmacology, University of North Carolina, School of Medicine, Chapel Hill, North Carolina 27599-7365, United States<sup>§</sup>Laboratory of Biological Modeling, NIDDK, National Institutes of Health, Bethesda, Maryland 20892, United States

## S Supporting Information

**ABSTRACT:** P2Y<sub>2</sub> and P2Y<sub>4</sub> receptors are G protein-coupled receptors, activated by UTP and dinucleoside tetraphosphates, which are difficult to distinguish pharmacologically for lack of potent and selective ligands. We structurally varied phosphate and uracil moieties in analogues of pyrimidine nucleoside 5'-triphosphates and 5'-tetraphosphate esters. P2Y<sub>4</sub> receptor potency in phospholipase C stimulation in transfected 1321N1 human astrocytoma cells was enhanced in N<sup>4</sup>-alkyloxycytidine derivatives. OH groups on a terminal  $\delta$ -glucose phosphoester of uridine 5'-tetraphosphate were inverted or substituted with H or F to probe H-bonding effects. N<sup>4</sup>-(Phenylpropoxy)-CTP **16** (MRS4062), Up<sub>4</sub>-[1]3'-deoxy-3'-fluoroglucose **34** (MRS2927), and N<sup>4</sup>-(phenylethoxy)-CTP **15** exhibit  $\geq 10$ -fold selectivity for human P2Y<sub>4</sub> over P2Y<sub>2</sub> and P2Y<sub>6</sub> receptors (EC<sub>50</sub> values 23, 62, and 73 nM, respectively).  $\delta$ -3-Chlorophenyl phosphoester **21** of Up<sub>4</sub> activated P2Y<sub>2</sub> but not P2Y<sub>4</sub> receptor. Selected nucleotides tested for chemical and enzymatic stability were much more stable than UTP. Agonist docking at CXCR4-based P2Y<sub>2</sub> and P2Y<sub>4</sub> receptor models indicated greater steric tolerance of N<sup>4</sup>-phenylpropoxy group at P2Y<sub>4</sub>. Thus, distal structural changes modulate potency, selectivity, and stability of extended uridine tetraphosphate derivatives, and we report the first P2Y<sub>4</sub> receptor-selective agonists.



## ■ INTRODUCTION

The eight subtypes of P2Y receptors are nucleotide-activated G protein-coupled receptors (GPCRs), and four of these subtypes, the P2Y<sub>2</sub>, P2Y<sub>4</sub>, P2Y<sub>6</sub>, and P2Y<sub>14</sub> receptors, respond to uracil nucleotides.<sup>1,2</sup> The P2Y<sub>2</sub> and P2Y<sub>4</sub> receptors are activated by uridine 5'-triphosphate (UTP, **1**, Chart 1) and its analogues and are difficult to distinguish pharmacologically, and a prominent need exists for definitive ligand tools.<sup>3,4</sup> The P2Y<sub>2</sub> receptor also is activated by analogues of adenine 5'-triphosphate.

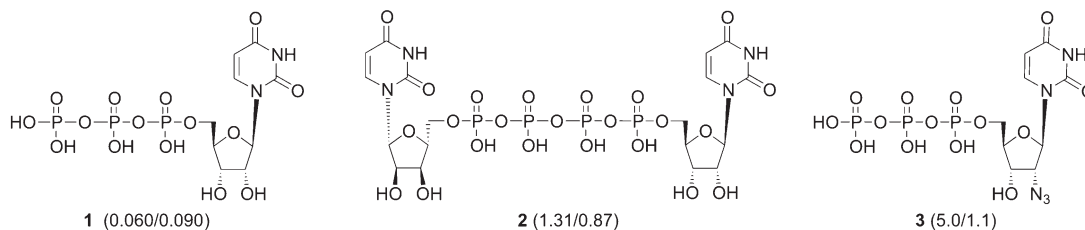
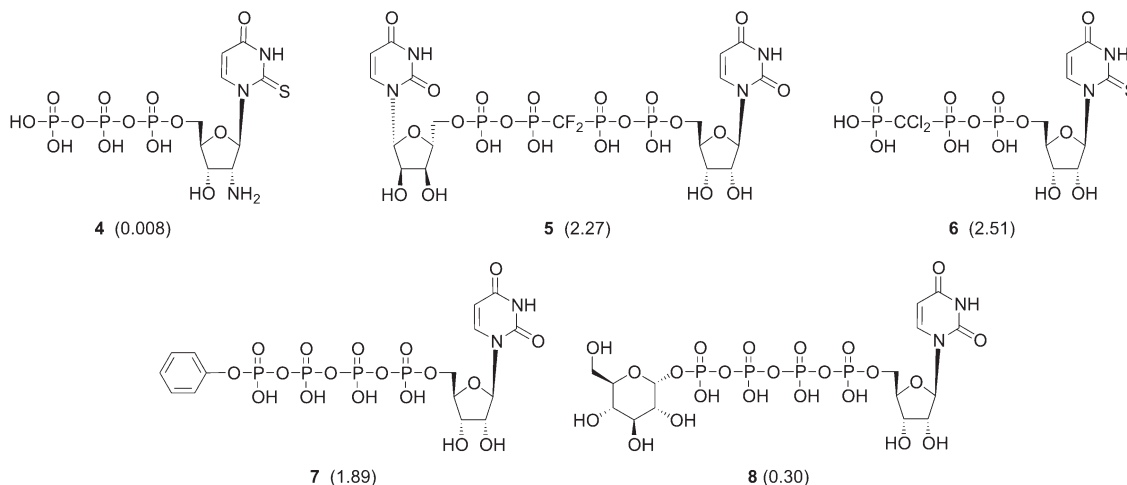
Dinucleotide P2Y<sub>2</sub> receptor agonists, such as **2** (Up<sub>4</sub>U, INS365), which are more resistant to enzymatic hydrolysis than **1**, are being developed clinically for the treatment of eye and pulmonary diseases.<sup>5–7</sup> Compounds **1** and **2** are not selective for the P2Y<sub>2</sub> receptor. However, several studies have explored the structure–activity relationship (SAR) of agonists<sup>8–13</sup> and antagonists<sup>14</sup> at the P2Y<sub>2</sub> receptor, and potent and selective P2Y<sub>2</sub> receptor agonists, such as **4** (MRS2698)<sup>10</sup> and C-linked nucleotides<sup>9</sup> have been identified. The nucleotide agonists **5–7** also are P2Y<sub>2</sub> receptor-selective relative to both P2Y<sub>4</sub> and P2Y<sub>6</sub>

receptors.<sup>13</sup> In contrast, the 2'-azido analogue **3** is one of the few analogues of **1** that displays any selectivity (only 5-fold in comparison to the P2Y<sub>2</sub> receptor) for the P2Y<sub>4</sub> receptor.<sup>8</sup> There are no selective antagonists of the P2Y<sub>4</sub> receptor.

In the present study, we further investigated SARs at the P2Y<sub>2</sub> and P2Y<sub>4</sub> receptors through synthesis of nucleotides with additional substitutions of the uracil and phosphate moieties and combinations thereof. These novel derivatives incorporated groups such as 4-methoxyimino and its homologues on the pyrimidine ring, found previously to enhance the potency of analogues of uridine 5'-diphosphate (UDP) at P2Y receptors.<sup>15</sup> We also probed the effects of substituting one uridine moiety of **2** with various sugar and aliphatic and aromatic alcohol moieties. Two lead  $\delta$ -phosphoesters of 5'-tetraphosphates that were recently reported as full agonists of the P2Y<sub>2</sub> receptor,<sup>13</sup> that is, **7** (MRS2768), which was P2Y<sub>2</sub> receptor-specific, and **8**

Received: December 15, 2010

Published: April 29, 2011

Chart 1. Structures and Potencies of Prototypical Agonist Ligands for Studying P2Y<sub>2</sub> and P2Y<sub>4</sub> ReceptorsP2Y<sub>2</sub>/P2Y<sub>4</sub> Receptor Agonists (EC<sub>50</sub> at P2Y<sub>2</sub>/P2Y<sub>4</sub>, μM)Selective P2Y<sub>2</sub> Receptor Agonists (EC<sub>50</sub>, μM)

(MRS2732), with 7- and 26-fold selectivity in comparison to P2Y<sub>4</sub> and P2Y<sub>6</sub> receptors, were modified in the present study. Although P2Y<sub>2</sub> receptor selectivity was not improved by these changes, several analogues exhibited important increases in potency and selectivity at the P2Y<sub>4</sub> receptor. This new chemical synthesis was combined with molecular docking studies based on a model derived from the recently solved structure of the CXCR4 chemokine receptor<sup>16</sup> to interrogate the molecular basis for selectivity of interaction of several of these molecules for the P2Y<sub>4</sub> receptor over the P2Y<sub>2</sub> receptor.

## RESULTS

**Chemical Synthesis.** Novel nucleotide derivatives (Table 1) were prepared by the synthetic routes shown in Schemes 1–6. The potencies of nine known reference compounds (**1**, **6–9**, **17–19**, and **27**) are also listed in Table 1.<sup>11–13</sup> The types of nucleotide modifications made included analogues of cytidine 5'-triphosphate (CTP) containing a N<sup>4</sup>-alkoxy group (Scheme 1), 5'-tetraphosphates derivatives of **17** (Up<sub>4</sub>) containing a substituted δ-phenyl phosphoester group at the terminal phosphate (Schemes 2 and 5), derivatives of **17** containing a sugar group at the terminal phosphate (Schemes 3 and 6), and analogues of **1** containing a β,γ-dichloromethylene-bridge in the triphosphate group (Scheme 4).

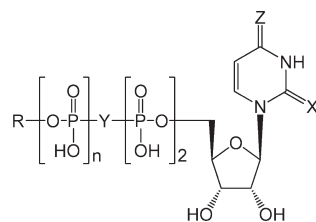
The synthesis of N<sup>4</sup>-alkoxy cytidines **39–42** from cytidine was performed using corresponding alkoxy amines. The resulting N<sup>4</sup>-alkoxy cytidines were phosphorylated by standard methods<sup>6</sup> to give the desired N<sup>4</sup>-alkoxy-CTP analogues **11–16** (Scheme 1). In each case, the unprotected nucleoside was first treated with

phosphorus oxychloride, and the reaction mixture was treated immediately with bis(tri-*n*-butylammonium) pyrophosphate to produce the 5'-triphosphate. The favored method for preparation of the β,γ-dichloromethylene derivative **10** was by condensation of dichloromethylenediphosphonic acid with uridine 5'-monophosphate (UMP) using *N,N'*-diisopropylcarbodiimide (DIC). An alternate method involving reaction with UMP-morpholide required 2 weeks of reaction to reach completion.

The synthesis of 5'-tetraphosphate derivatives that were modified at the terminal phosphates was performed using a carbodiimide coupling reagent in the presence of magnesium chloride (Schemes 5 and 6). The addition of MgCl<sub>2</sub> dramatically increased the reactivity during the coupling reaction of monophosphate and triphosphate,<sup>17</sup> but it impeded the coupling of monophosphate and diphosphate (data not shown). Phenyl monophosphates **57–62** were prepared by phosphorylation with a dibenzyl-protected phosphate group followed by deprotection of the benzyl groups using trimethylsilyl bromide (TMS-Br, Scheme 2).<sup>15</sup> Hexose sugar monophosphates **68–72** were phosphorylated at the 1'-position by full acetylation and treatment with phosphoric acid. The synthesis of glucuronic acid-1-monophosphate **74** was performed by oxidation of commercially available glucose-1-monophosphate using 2,2,6,6-tetramethylpiperidine-1-oxyl (TEMPO) as a catalyst.<sup>18</sup>

**Pharmacological Activity.** The activation of phospholipase C (PLC) by a range of concentrations of each newly synthesized nucleotide derivative (**10–37**) was studied in [<sup>3</sup>H]inositol-labeled 1321N1 human astrocytoma cells stably expressing the human P2Y<sub>2</sub>, P2Y<sub>4</sub>, or P2Y<sub>6</sub> receptor by following the

**Table 1. Relative Potencies of 1 and Its Analogues for Activation of the Human P2Y<sub>2</sub>, P2Y<sub>4</sub>, and P2Y<sub>6</sub> Receptors (Unless Noted: R = H; X, Y = O; and Z = O)**



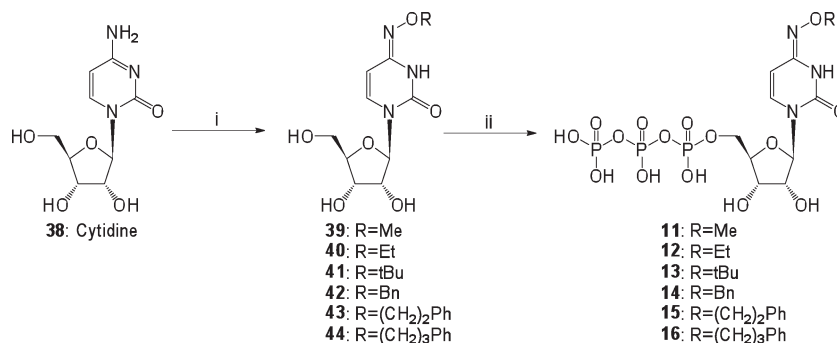
Com- pound	Modification	Structure	EC <sub>50</sub> , nM <sup>a</sup>		
			hP2Y <sub>2</sub>	hP2Y <sub>4</sub>	hP2Y <sub>6</sub>
<b>TRIPHOSPHATES (n = 1)</b>					
1 <sup>b</sup>	(= UTP)		55 ± 4	80 ± 8	>10,000 <sup>d</sup>
6 <sup>b</sup>	2-thio-β,γ-CCl <sub>2</sub> -UTP	X = S, Y = CCl <sub>2</sub>	2510 ± 650	NE	NE
9 <sup>b</sup>	2-thio-UTP	X = S	35 ± 4	350 ± 100	~1500
10 <sup>b</sup>	β,γ-CCl <sub>2</sub> -UTP	Y = CCl <sub>2</sub>	9600 ± 2100	NE	≤50% at 10 μM
11	N <sup>4</sup> -OMe-CTP	Z = N-OCH <sub>3</sub>	28 ± 4	25 ± 3	130 ± 21
12	N <sup>4</sup> -OEt-CTP	Z = N-OCH <sub>2</sub> CH <sub>3</sub>	817 ± 93	210 ± 79	877 ± 50
13	N <sup>4</sup> -OBu-CTP	Z = N-OC(CH <sub>3</sub> ) <sub>3</sub>	1500 ± 240	2110 ± 680	≤50% at 10 μM
14	N <sup>4</sup> -OBn-CTP	Z = N-OCH <sub>2</sub> Ph	620 ± 75	97 ± 14	230 ± 37
15	N <sup>4</sup> -OEtPh-CTP	Z = N-O(CH <sub>2</sub> ) <sub>2</sub> Ph	1200 ± 270	73 ± 17	1210 ± 220
16	N <sup>4</sup> -OPrPh-CTP	Z = N-O(CH <sub>2</sub> ) <sub>3</sub> Ph	640 ± 147	23 ± 4	740 ± 29
<b>TETRAPHOSPHATES (n = 2)</b>					
17 <sup>b</sup>	Up <sub>4</sub>		3900 ± 1200	7300 ± 1600	7600 ± 1100
18 <sup>b</sup>	Up <sub>4</sub> -OMe	R = CH <sub>3</sub>	4000 ± 510	2700 ± 430	>10,000 <sup>d</sup>
19 <sup>b</sup>	Up <sub>4</sub> -O(CH <sub>2</sub> ) <sub>2</sub> CN	R = (CH <sub>2</sub> ) <sub>2</sub> CN	1700 ± 220	1960 ± 530	>10,000 <sup>d</sup>
7	Up <sub>4</sub> -OC <sub>6</sub> H <sub>5</sub>	R =	2760 ± 630	NE	NE
20	Up <sub>4</sub> -OC <sub>6</sub> H <sub>4</sub> (4-Cl)	R =	6600 ± 1600	c	c
21	Up <sub>4</sub> -OC <sub>6</sub> H <sub>4</sub> (3-Cl)	R =	840 ± 50	NE	3690 ± 750
22	Up <sub>4</sub> -OC <sub>6</sub> H <sub>4</sub> (4-OMe)	R =	≤50% at 10 μM	≤50% at 10 μM	≤50% at 10 μM
23	Up <sub>4</sub> -OC <sub>6</sub> H <sub>4</sub> (3-OMe)	R =	≤50% at 10 μM	NE	≤50% at 10 μM
24	Up <sub>4</sub> -OC <sub>6</sub> H <sub>4</sub> (4-NO <sub>2</sub> )	R =	4850 ± 1000	≤50% at 10 μM	≤50% at 10 μM
25	Up <sub>4</sub> -OC <sub>6</sub> H <sub>4</sub> (3-NO <sub>2</sub> )	R =	3330 ± 620	2540 ± 460	≤50% at 10 μM
<b>TETRAPHOSPHATE SUGAR DERIVATIVES (n = 2)</b>					
2 <sup>b</sup>	Up <sub>4</sub> U	R = [5]uridine	210 ± 30	130 ± 10	1160 ± 420
8 <sup>b</sup>	Up <sub>4</sub> -[1]glucose	R =	300 ± 130	2060 ± 180	7830 ± 170
26	β,γ-dichloromethylene - Up <sub>4</sub> -[1]glucose	R = Y = CCl <sub>2</sub>	≤50% at 10 μM	NE	NE
27 <sup>b</sup>	Up <sub>4</sub> -[1]galactose	R =	940 ± 120	1770 ± 410	8190 ± 730

Table 1. Continued

Compound	Modification	Structure	EC <sub>50</sub> , nM <sup>a</sup>		
			hP2Y <sub>2</sub>	hP2Y <sub>4</sub>	hP2Y <sub>6</sub>
28	Up <sub>4</sub> -[1]jallose		770 ± 220	183 ± 9	1170 ± 130
29	Up <sub>4</sub> -[1]mannose		3720 ± 1140	4480 ± 620	12,100 ± 2450
30	Up <sub>4</sub> -[1]xylose		2770 ± 560	620 ± 30	4900 ± 660
31	Up <sub>4</sub> -[1]2'-deoxy-2'-acetamidoglucose		1890 ± 400	910 ± 100	5460 ± 860
32	Up <sub>4</sub> -[1]glucuronic acid		490 ± 44	227 ± 88	1650 ± 340
33	Up <sub>4</sub> -[1]2'-deoxy-2'-fluoroglucose		≤50% at 10 μM	≤50% at 10 μM	≤50% at 10 μM
34	Up <sub>4</sub> -[1]3'-deoxy-3'-fluoroglucose		710 ± 120	62 ± 19	950 ± 150
35	N <sup>4</sup> -OBn-Cp <sub>4</sub> -[1]3'-deoxy-3'-fluoroglucose		2640 ± 588	670 ± 100	7510 ± 240
36	N <sup>4</sup> -OMe-Cp <sub>4</sub> -[1]3'-deoxy-3'-fluoroglucose		500 ± 62	310 ± 13	1440 ± 280
37	Up <sub>4</sub> -[1]4'-deoxy-4'-fluoroglucose		620 ± 220	220 ± 30	1640 ± 140

<sup>a</sup> Agonist potencies reflect stimulation of PLC in 1321N1 human astrocytoma cells stably expressing the human P2Y<sub>2</sub>, P2Y<sub>4</sub>, or P2Y<sub>6</sub> receptor. Potencies are presented in the form of EC<sub>50</sub> values, which represent the concentration of agonist at which 50% of the maximal effect is achieved. These values were determined using a four-parameter logistic equation and the GraphPad software package (GraphPad, San Diego, CA). The results are presented as means ± standard errors and are the average of 3–6 different experiments with each molecule. <sup>b</sup> Agonist potencies for compounds **2**, **6**, **8**, **9**, **18**, and **19** were from published reports.<sup>8,13</sup> Compounds **1**, **7**, **10**, **17**, and **27** were reported in Ko et al.<sup>13</sup> but reassayed in this study. <sup>c</sup> Not determined. <sup>d</sup> ≤50% effect at 10 μM. Values of >10 μM were determined by extrapolation. NE=no effect at 10 μM.

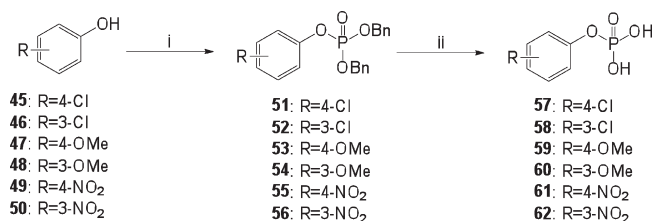
### Scheme 1. Synthesis of Alkoxyimino Derivatives<sup>a</sup>



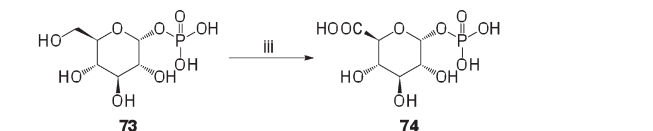
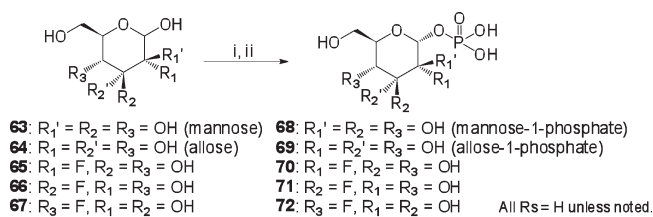
<sup>a</sup> Reagents and conditions: (i) RONH<sub>2</sub>, pyridine, 100 °C, overnight. (ii) (a) Proton Sponge, POCl<sub>3</sub>, PO(OMe)<sub>3</sub>, 0 °C, 3 h; (b) Bu<sub>3</sub>N, tributylammonium pyrophosphate, 0 °C, 10 min; (c) triethylammonium bicarbonate(aq), room temperature, 30 min.

methodology (see the Experimental Section) that we described previously in detail.<sup>13,15,19</sup>

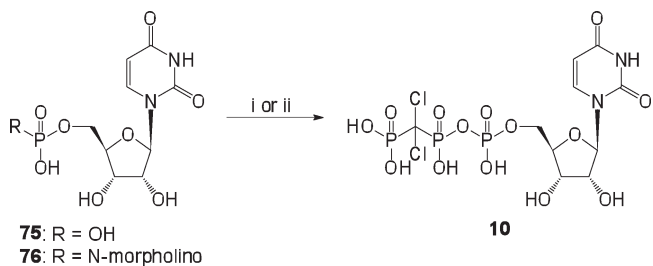
Table 1 illustrates analogues of **1** and **17** that were designed for possible interaction with the P2Y<sub>2</sub> and P2Y<sub>4</sub> receptors and their

Scheme 2. Synthesis of Aryl Phosphates<sup>a</sup>

<sup>a</sup> Reagents and conditions: (i) CBr<sub>4</sub>, iPr<sub>2</sub>NEt, dibenzyl phosphite, MeCN, room temperature, 2 h. (ii) TMS-Br, CH<sub>2</sub>Cl<sub>2</sub>, room temperature, 1.5 h.

Scheme 3. Synthesis of Sugar-1-phosphates<sup>a</sup>

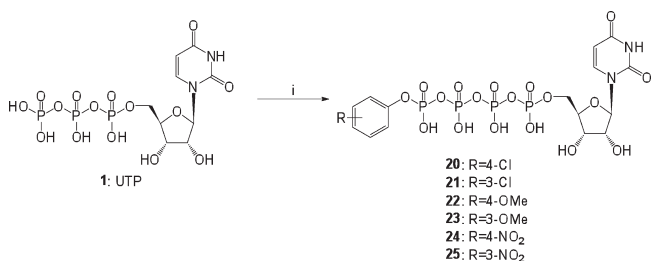
<sup>a</sup> Reagents and conditions: (i) Ac<sub>2</sub>O, NaOAc, 5 h, 110 °C. (ii) H<sub>3</sub>PO<sub>4</sub>, 50 °C, 3 h. (iii) TEMPO, H<sub>2</sub>O, NaOH, NaOCl, 0 °C.

Scheme 4. Synthesis of β,γ-Dichloromethylene-UTP 10<sup>a</sup>

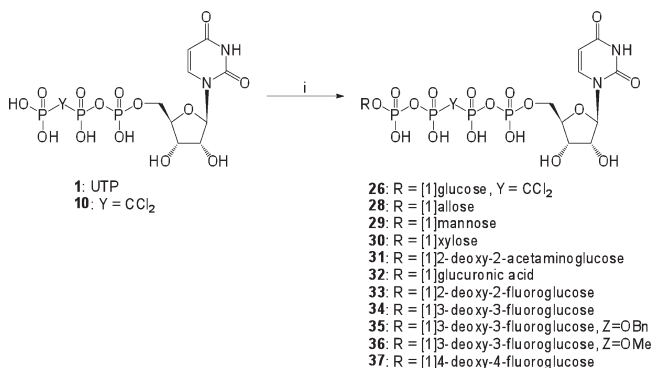
<sup>a</sup> Reagents and conditions: From 75, (i) (a) DIC, DMF, room temperature, 3 h; (b) PO(OH)<sub>2</sub>CCl<sub>2</sub>PO(OH)<sub>2</sub>, MgCl<sub>2</sub>, DMF, room temperature, overnight. From 76, (ii) PO(OH)<sub>2</sub>CCl<sub>2</sub>PO(OH)<sub>2</sub>, DMF, room temperature, 2 weeks.

biological potencies. Introduction of β,γ-phosphonomethylene bridges, which enhance the stability of nucleotides against the action of ectonucleotidases, resulted in compounds 6 and 10 that were inactive at the P2Y<sub>4</sub> receptor.<sup>13</sup>

The possibility of a hydrophobic pocket beyond the 4-position of the pyrimidine ring in the P2Y<sub>2</sub> or P2Y<sub>4</sub> receptor structure was probed in analogues of 1 with N<sup>4</sup>-alkoxyimino moieties 11–16. One of these molecules, N<sup>4</sup>-methoxy-CTP 11,<sup>15</sup> was more potent than the native ligand 1 at both subtypes. Within a related series of homologous arylalkoxy derivatives, the N<sup>4</sup>-phenylpropoxy substitution of CTP in 16 was found to optimally increase activity at the P2Y<sub>4</sub> receptor with an EC<sub>50</sub> value of 23 nM (Figures 1 and 2). This compound displayed selectivities of

Scheme 5. Synthesis of Up<sub>4</sub>-δ-phenyl Ester Derivatives<sup>a</sup>

<sup>a</sup> Reagents and conditions: (i) (a) DIC, DMF, room temperature, 3 h; (b) aryl-1-phosphate, MgCl<sub>2</sub>, DMF, room temperature, overnight.

Scheme 6. Synthesis of Up<sub>4</sub>-δ-sugar Derivatives<sup>a</sup>

<sup>a</sup> Reagent and conditions: (i) (a) DIC or DCC, DMF, room temperature, 3 h; (b) sugar-1-phosphate, MgCl<sub>2</sub>, DMF, room temperature, 2 h to overnight. Unless noted, Y = O.

28- and 32-fold in comparison to the P2Y<sub>2</sub> and P2Y<sub>6</sub> receptors, respectively. N<sup>4</sup>-Phenylethoxy substitution of CTP resulted in a molecule 15 that exhibited somewhat lower potency (EC<sub>50</sub> = 73 nM) and selectivity (16- and 17-fold in comparison to the P2Y<sub>2</sub> and P2Y<sub>6</sub> receptors, respectively) than 16 for the P2Y<sub>4</sub> receptor.

Introduction of either a sugar moiety or a substituted phenyl ring at the terminal δ-phosphate was examined in the series of S'-tetraphosphates. We previously reported that introduction of a glucose or phenyl ester group at the δ-phosphate resulted in increased selectivity for the P2Y<sub>2</sub> receptor against the P2Y<sub>4</sub> and P2Y<sub>6</sub> receptors.<sup>13</sup> A 3-Cl derivative 21 showed higher potency than the phenyl derivative 7, but its P2Y<sub>2</sub> receptor selectivity in comparison to the P2Y<sub>6</sub> receptor was decreased. Similarly, all substitutions of the δ-phenyl ester examined (20–25) were either less potent or less selective for the P2Y<sub>2</sub> receptor than the unsubstituted 7.

Consistent with previous findings, introduction of a β,γ-dichloromethylene substitution in 24 abolished activity at the three P2Y receptors tested. On the basis of the P2Y<sub>2</sub> receptor selectivity of Up<sub>4</sub>-δ-[1]glucose 8,<sup>13</sup> substitutions of the δ-glucose moiety were examined (26–37). The types of glucose modifications included were inversion of hydroxyl groups (27–29), replacement of a hydroxyl group with F (33–37), and other omission or other replacement of hydroxyl functionality (30–32). These modifications resulted in greatly varied potency and selectivity for the P2Y receptors. Inversion of the 3'-hydroxyl group in the allose derivative 28 increased P2Y<sub>4</sub> receptor potency 11-fold, but inversion of the 2'-hydroxyl group in the mannose derivative 29 decreased potency at P2Y<sub>2</sub>, P2Y<sub>4</sub>, and P2Y<sub>6</sub>

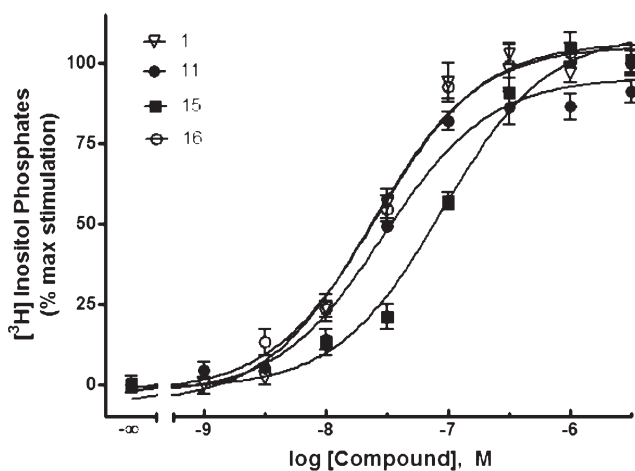


**Figure 1.** Activity of native agonist **1** and alkyloxyimino derivatives **11**, **15**–**16** at the P2Y<sub>4</sub> receptor as indicated by activation of PLC in 1321N1 human astrocytoma cells stably expressing the human P2Y<sub>4</sub> receptor.

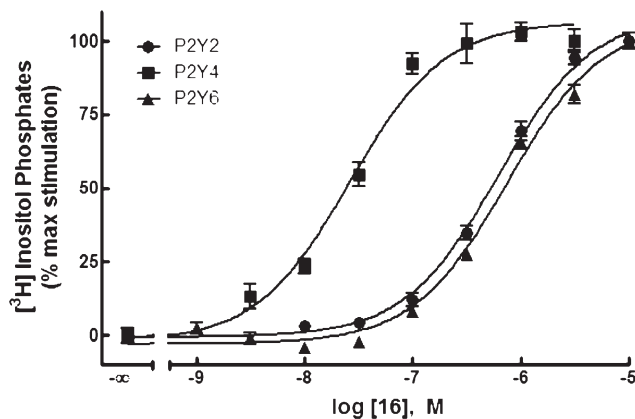


**Figure 2.** Activity of compound **16** [*N*<sup>4</sup>-(phenylpropoxy)-CTP] at P2Y<sub>2</sub>, P2Y<sub>4</sub>, and P2Y<sub>6</sub> receptors as indicated by activation of PLC in 1321N1 human astrocytoma cells stably expressing the human P2Y<sub>2</sub>, P2Y<sub>4</sub>, or P2Y<sub>6</sub> receptor. The effect of **1** corresponds to 100%.

receptors. Fluoro substitution at the 2'-position of the terminal  $\delta$ -glucose moiety in **33** greatly reduced activity at all three receptor subtypes, suggesting that the H-bond-donating property of the 2'-hydroxyl group is necessary for this biological activity. The hydroxymethylene group appeared to be important for activity at the P2Y<sub>2</sub> receptor, because the xylose derivative **30** exhibited reduced activity (9-fold less potent than **8**) at this subtype.

The 3'- and 4'-fluoro derivatives **34** and **37** maintained activity at the P2Y<sub>2</sub> receptor. However, fluoro substitution at the 3'-position of the terminal glucose moiety in **34** greatly increased potency ( $EC_{50} = 62$  nM) at the P2Y<sub>4</sub> receptor. Thus, P2Y<sub>4</sub> receptor selectivities of 11.5- and 15.3-fold were observed for this analogue in comparison to the P2Y<sub>2</sub> and P2Y<sub>6</sub> receptors, respectively. Analogues **35** and **36** that included combination of 3'-deoxy-3'-fluoroglucose with the *N*<sup>4</sup>-benzyloxyimino or *N*<sup>4</sup>-methoxyimino modification in the nucleobase were less active and selective than unmodified **34**. Thus, simultaneous introduction of these two P2Y<sub>4</sub> receptor-directing modifications did not produce further enhancement of potency or selectivity.

**Molecular Modeling.** In light of the SAR data generated through this work, in particular the different selectivity profile of compounds **11** and **16**, we revised our experimentally supported modeling hypothesis for the binding model of pyrimidine-based nucleotides to the P2Y<sub>2</sub> and P2Y<sub>4</sub> receptors, through the incorporation of further experimental data. These new models were not used to design the compounds but to offer a putative structural interpretation of the results. Note that to facilitate the comparison among receptors, throughout this section, amino acid residues are designated both with their residue number in the P2Y<sub>2</sub> and P2Y<sub>4</sub> sequence and the universal GPCR residue identifier defined by the Ballesteros and Weinstein.<sup>20,28,29</sup>

In the absence of experimentally elucidated structures of any of the members of the P2Y family, in the past decade, we have constructed models of the P2Y<sub>2</sub> and P2Y<sub>4</sub> receptors through homology modeling based on rhodopsin, which, at the time, was the only crystallographically solved GPCR, followed by molecular docking.<sup>8,10,20</sup> We incorporated into the models several hypotheses derived from experiments. These included the presence of two disulfide bridges and a salt bridge that putatively contributes to the shape of the extracellular domains of the receptors. Data from mutagenesis studies revealed that the residues involved in the formation of these extracellular bridges are fundamental to the function of P2Y receptors.<sup>22–24</sup> The binding mode of the ligand was also driven by mutagenesis and SAR data. Specifically, our published models were constructed using as anchors for the binding of the phosphate moieties of the nucleotides three cationic residues located in transmembrane  $\alpha$ -helix 3 (TM3), TM6, and TM7 that are essential for ligand recognition according to mutagenesis data.<sup>24–26</sup> The Northern (N) conformation adopted by the ribose moiety of **1** and the orientation of the nucleobase toward the opening of the interhelical cavity are also supported by SAR data.<sup>11,15,21,30</sup>

Our rhodopsin-based models do not explain the different selectivity profiles of compounds **11** and **16**, because in those models the area that surrounds the *N*<sup>4</sup> substituents of the two compounds is completely conserved between the P2Y<sub>2</sub> and the P2Y<sub>4</sub> receptors (Figure 3). Here, we propose revised models of the P2Y<sub>2</sub> and P2Y<sub>4</sub> receptors that incorporate the experimentally supported features of the previous models and are consistent with SAR data gathered in this work. The new models are based on the recently solved X-ray crystal structure of the CXCR4 chemokine receptor,<sup>16</sup> which, among all of those currently available, is the closest to the P2Y receptors.<sup>20</sup> Among the crystallographically solved GPCRs, this receptor shares the highest sequence similarity with P2Y receptors, showing 24.6 and 25.7% of sequence identity with the P2Y<sub>2</sub> and the P2Y<sub>4</sub> receptor—the sequence identity was calculated according to the alignment shown in Figure 4 and refers to the entire portion of the CXCR4 receptor that was solved crystallographically, with the exclusion of the C-terminal domain. Moreover, the CXCR4 contains a disulfide bridge, putatively present also in the P2Y<sub>2</sub> and P2Y<sub>4</sub> receptors, connecting the N-terminus (through a Cys located two positions upstream when compared to the P2Ys) with the boundary between extracellular loop 3 (EL3) and TM7 (through a Cys located at position 7.25, as in the P2Y receptors)—see Figure 4. Before the solution of the CXCR4 structure, none of the structurally characterized GPCRs featured a similar disulfide bridge. Like the previous rhodopsin-based models, our current models incorporate all of the experimentally derived structural features mentioned above, including the aforementioned pair of extracellular disulfide bridges and the salt bridge connecting EL2

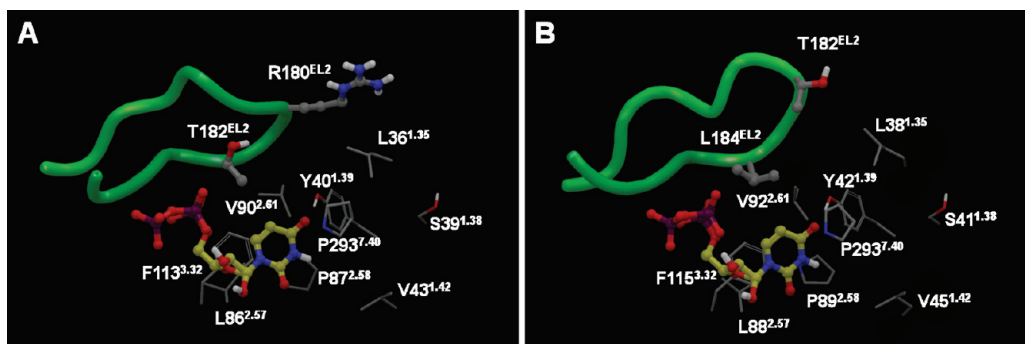


**Figure 3.** Rhodopsin-based molecular models of the P2Y<sub>2</sub> and P2Y<sub>4</sub> receptors.<sup>8</sup> The second EL (EL2) is schematically represented as a green tube. The area that in these models would surround the N<sup>4</sup> substituents of the imino derivatives described in this article, is completely conserved between the P2Y<sub>2</sub> and the P2Y<sub>4</sub> receptor. This is in contrast with the fact that large N<sup>4</sup> substituents are better tolerated by the P2Y<sub>4</sub> than the P2Y<sub>2</sub> receptor. Two nonconserved EL2 residues that could explain the selectivity profile of the N<sup>4</sup> substituted compounds according to the CXCR4 models (see Figure 5) are not positioned in a way that would allow interactions with such moieties in the rhodopsin-based models. Receptor residues are represented with gray carbons, while ligands are represented with yellow carbons. See the figure of Jacobson et al. in ref 8 for further details on the rhodopsin-based models.



**Figure 4.** Sequence alignment of CXCR<sub>4</sub>, P2Y<sub>2</sub>, and P2Y<sub>4</sub> receptors used for the construction of the homology models. The sequence of the P2Y<sub>1</sub> receptor, on which most of the mutagenesis studies were performed, is also shown. Green dots indicate the two nonconserved EL2 residues putatively responsible for the selectivity of compound 16 for the P2Y<sub>4</sub> receptor. Blue dots indicate the conserved cationic residues putatively responsible for coordination of the negatively charged phosphate groups of the ligands. An additional cationic residue, Lys289<sup>7-36</sup> of the P2Y<sub>4</sub> receptor, is proposed to interact with the  $\alpha$ -phosphate. The cysteine residues involved in the formation of disulfide bridges are encased in a dark yellow box and connected by a dark yellow line. The glutamate and arginine residues involved in the formation of the salt bridge that putatively connects EL2 to the extracellular end of TM6, conserved also in the P2Y<sub>1</sub> receptor, are encased in a red and a blue box, respectively, and are connected by a red and blue line. The secondary structure of the template is indicated by a color-coded bar, with  $\alpha$ -helices in red,  $\beta$ -strands in yellow, and turns in blue. For each TM, black dots indicate the X.50 position, as defined in the GPCR indexing system. Transmembrane helices (TMs), extracellular loops (ELs), and intracellular loops (ILs) are indicated by labels. The figure was generated with MOE.<sup>40</sup>

with the extracellular end of TM6. These features, contribute to shaping of the opening of the interhelical cavity lined by residues

located in the extracellular N-terminus, the three ELs, and all of the TMs (Figure 5).

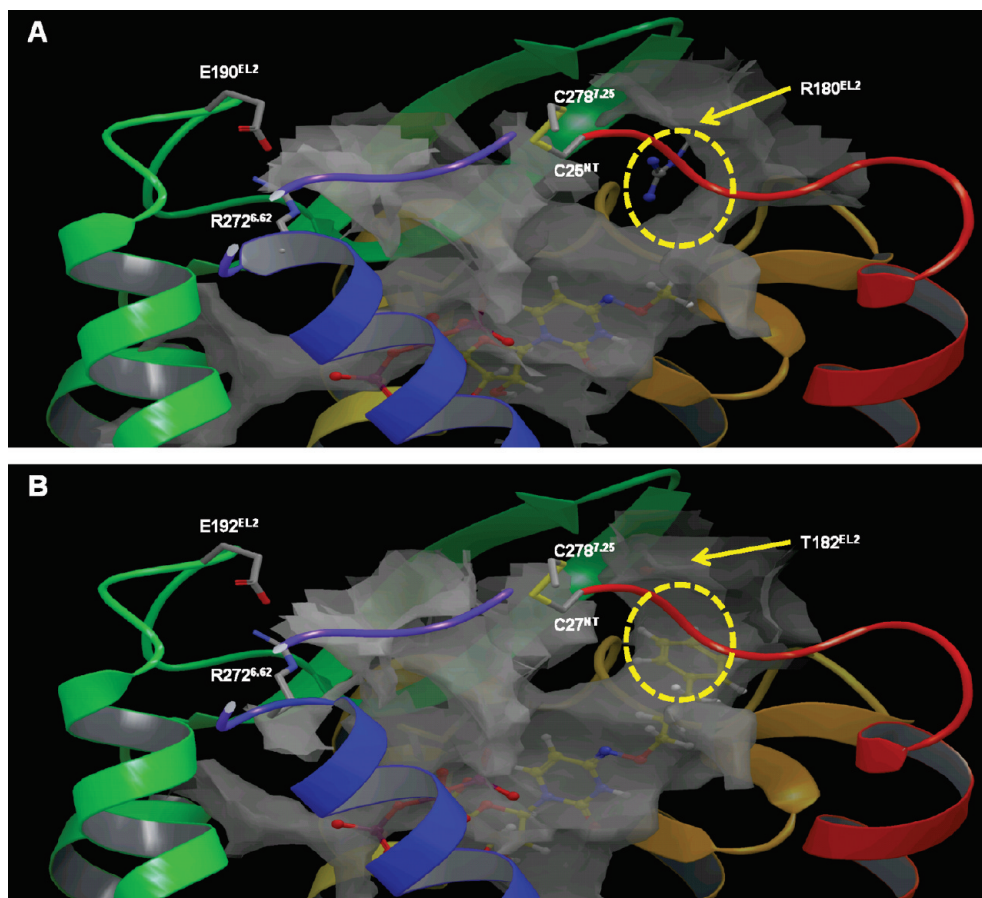


**Figure 5.** Contour of the interhelical cavity (in gray) of the P2Y<sub>2</sub> and P2Y<sub>4</sub> receptor deduced from the analysis of the new CXCR4 homology models. According to these models, there is only one region, indicated by a dashed yellow circle, where the cavity is significantly smaller in the P2Y<sub>2</sub> than in the P2Y<sub>4</sub> receptor. This difference is due to a nonconserved amino acid in EL2, which is a threonine (Thr182) in the P2Y<sub>4</sub> receptor and a bulkier arginine (Arg180) in the P2Y<sub>2</sub> receptor. Of note, an arginine residue is present at the corresponding position of the CXCR4 receptor (Arg183). The orientation of Arg180 in our model of the P2Y<sub>2</sub> receptor follows the orientation of Arg183 in the crystal structure of the CXCR4 receptor. The disulfide bridge that putatively links the N-terminus with EL3 and the salt bridge that putatively links TM6 with EL2 are shown. The disulfide bridge that links TM3 with EL2 is not clearly visible because it is obscured by the interhelical cavity. Compounds **11** and **16** are shown within the pockets of the P2Y<sub>2</sub> and P2Y<sub>4</sub> receptors, respectively. The backbone of the receptor is schematically represented as a ribbon colored with a continuum spectrum going from red, at the N-terminus, to purple, at the C-terminus. For convenience, TM7 is not shown.

We used the new CXCR4-based *in silico* structures of the P2Y<sub>2</sub> and P2Y<sub>4</sub> receptors to construct models of the putative complexes of the two receptors with compounds **11** and **16**. Importantly, we incorporated in the binding mode and in the conformation of the two ligands all of the experimentally supported features shown in our previous models.<sup>8,10,20</sup> Moreover, we incorporated novel experimental information that we gathered through NMR spectroscopy and X-ray crystallography. Specifically, the tautomeric form of the imino group and its conformation were determined through NMR spectroscopy (chemical shift of NH at 3-position of **39** and nuclear Overhauser effect between MeO and NH). Additionally, an X-ray crystallographic structure was obtained for N<sup>4</sup>-*t*-BuO-cytosine (Supporting Information), which is in close agreement with a literature report for N<sup>4</sup>-MeO-cytosine.<sup>27</sup> The data clearly showed the presence of a hydrogen atom at the 3-position and the absence of a hydrogen atom at the N<sup>4</sup>-position. Bond lengths also indicate that the compound adopts an exo double bond tautomeric form.

Interestingly, the new models show several distinctive features that make them compatible with the selectivity profile of compounds **11** and **16** for the P2Y<sub>2</sub> and P2Y<sub>4</sub> receptors. Specifically,

the binding of nucleotides appears shifted toward the extracellular side in the new CXCR4-based models as compared to those previously reported (Figure 6).<sup>8,10,20</sup> This is due to the fact that in the new models the side chain of Phe<sup>3.32</sup> (113 for P2Y<sub>2</sub>, 115 for P2Y<sub>4</sub>)—a residue common to all P2Y receptors and conserved as an aromatic residue (Tyr116<sup>3.32</sup>) in the CXCR4 receptor—is parallel to the plane of the membrane. Because of this orientation, which is consistent with the one shown by Tyr116<sup>3.32</sup> in the crystal structure of the CXCR4 receptor, Phe<sup>3.32</sup> limits the depth of the binding cavity and prevents the ligands from docking at a position more distal to the extracellular side. Our previous models, which were built prior to the availability of a template containing an aromatic residue at position 3.32, featured the side chain of Phe<sup>3.32</sup> oriented perpendicularly to the plane of the membrane and in  $\pi$ -stacking with the nucleobase of the ligands and allowed for a deeper binding pocket.<sup>8,10,20</sup> Because of the shallower binding mode proposed here in comparison to our previous rhodopsin-based models, the CXCR4-based models are compatible with the influence of the substituent at position 4 of the pyrimidine ring profile of compounds of the newly synthesized alkoxyimino derivatives on their selectivity for the P2Y<sub>4</sub>



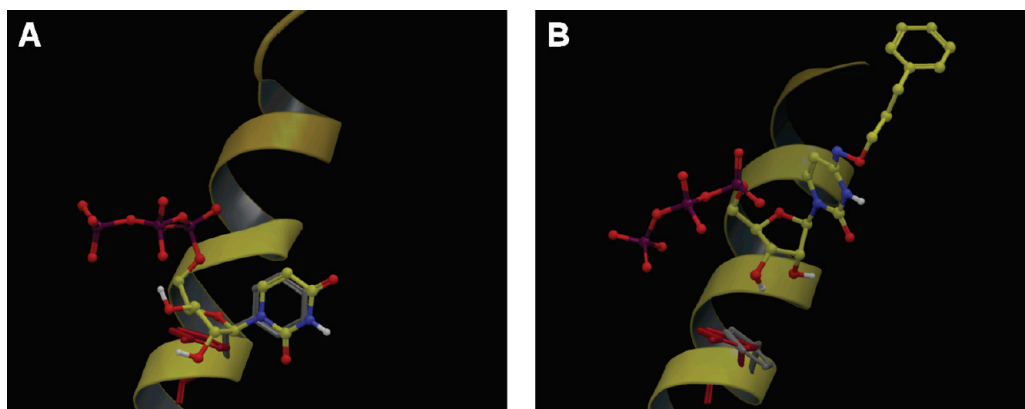


**Figure 6.** Previously published rhodopsin-based model (A, in complex with **1**) and new CXCR4-based model of the P2Y<sub>4</sub> receptor (B, in complex with **16**). One residue of the CXCR4 receptor (Tyr116<sup>3,32</sup>, in red) was key to deduce the putative rotameric state of the corresponding residue in the P2Y<sub>2</sub> and P2Y<sub>4</sub> receptors (Phe113<sup>3,32</sup> for P2Y<sub>2</sub> and Phe115<sup>3,32</sup> for P2Y<sub>4</sub>, in gray) in the new models. The CXCR4-based rotameric state of Phe<sup>3,32</sup> caused a significant change of the ligand binding mode with respect to the previously published one. The backbone of TM3 is schematically represented as a yellow ribbon.

versus the P2Y<sub>2</sub> receptor (Figure 5). In particular, the phenyl moiety of the N<sup>4</sup> substituent of compound **16** protrudes toward EL2, fitting into a cavity lined by two EL2 residues, namely, Thr182 and Leu184 in the P2Y<sub>4</sub> receptor. These two residues are not conserved in the P2Y<sub>2</sub> receptor, where their place is taken by Arg180 and Thr182, respectively. Our models suggest that these differences may account for the P2Y<sub>4</sub> receptor selectivity of **16**, especially in light of the fact that the sterically bulky Arg180, conserved in the CXCR4 receptor and oriented as in the CXCR4 crystal structure, seems to considerably reduce the volume of the cavity of the P2Y<sub>2</sub> receptor. As evident from Figure 5, this is the only region of the interhelical cavity that shows a significantly smaller volume in the P2Y<sub>2</sub> than in the P2Y<sub>4</sub> receptor.

**Stability of Nucleotide Derivatives.** Chemical and enzymatic instability of nucleotide analogues in biological systems is a major limitation in their use as pharmacological probes. Therefore, selected nucleotide derivatives were evaluated for stability during prolonged exposure to two different conditions. The derivatives were incubated at 37 °C in aqueous medium at either low pH or in the presence of membranes prepared from 1321N1 human astrocytoma cells,<sup>15</sup> which contain ectonucleotidases and are representative of cells of the mammalian central nervous system. At regular intervals, aliquots were taken for high-performance liquid chromatography (HPLC) analysis (Figure 7).

All of the nucleotide analogues tested were more stable in the presence of cell membranes than the native agonist **1**, and the most stable in the group was the Up<sub>4</sub>- $\delta$ -phenyl ester **7**. The 4-chlorophenyl analogue **20** appeared to be more stable than the corresponding 4-methoxy **22** and 4-nitro **24** analogues. Among the nucleotide analogues tested, only Up<sub>4</sub>-[1]glucose **8** was less stable at pH 1.5 than **1**. In general, the Up<sub>4</sub>- $\delta$ -phenyl esters displayed a relatively high degree of stability under both conditions in comparison to **1**. The stability at pH 1.5 was also determined for the potent P2Y<sub>4</sub> receptor agonists **15**, **16**, and **34**. The 5'-triphosphate derivatives **15** and **16** were similar in stability to **1**, and **34** was much more labile, similar to the closely related  $\delta$ -glucose phosphoester **8** (Supporting Information).

## DISCUSSION

Pharmacological resolution of responses mediated by P2Y<sub>2</sub> versus P2Y<sub>4</sub> receptors has been problematic due to lack of selective

antagonists and the fact that many analogues of **1** and diuridine tetraphosphates activate both subtypes. Two classical, general antagonists for P2 receptors, suramin and Reactive Blue 2, have been used as slightly selective antagonists of the P2Y<sub>2</sub> and P2Y<sub>4</sub> receptors, respectively.<sup>4,31,32</sup> In the rat, inosine-5'-triphosphate was shown to be 13-fold selective as an agonist at the P2Y<sub>4</sub> receptor in comparison to the P2Y<sub>2</sub> receptor.<sup>32</sup> The work described here identifies modifications that provide important new directions for introduction of agonist selectivity for P2Y<sub>4</sub> receptor ligands.

The P2Y<sub>4</sub> receptor is often expressed in the same tissues or, in some cases, the same cells as the widely distributed P2Y<sub>2</sub> receptor. This is the case for epithelial cells of the intestine. The study of knockout mice has revealed that the stimulatory effect of **1** on chloride secretion is mediated by the P2Y<sub>4</sub> receptor,<sup>33,34</sup> whereas its inhibitory effect on sodium absorption involves the P2Y<sub>2</sub> receptor.<sup>35</sup> Protective effects of P2Y<sub>4</sub> receptor activation were observed during cardiac ischemia studied in murine HL-1 myocytes.<sup>36</sup> P2Y<sub>4</sub> mRNA is expressed in microvascular endothelial cells isolated from mouse heart but not lung.<sup>37</sup> The effects of **1** on migration, proliferation, and VCAM-1 expression in these cells were greatly reduced in P2Y<sub>4</sub> receptor-deficient mice.<sup>37</sup> Macrophage adhesion induced by **1** also was reduced, and P2Y<sub>4</sub> receptor-null mice displayed defective angiogenesis in *in vivo* models.<sup>37</sup> In contrast, P2Y<sub>2</sub> receptor-deficient mice exhibit reduced effects of **1** on leukocyte adhesion, eosinophil migration, and VCAM-1 expression.<sup>38</sup> Thus, selective P2Y<sub>4</sub> receptor agonists might prove useful in the treatment of constipation, cardiac ischemia, or inflammation and exhibit reduced proinflammatory effects in the lung due to lack of interaction with the P2Y<sub>2</sub> receptor.

Substitutions at the 4-position of the nucleobase were explored through the synthesis of imino derivatives of various sizes. The exploration of this region, done through a classic medicinal chemistry approach, was prompted by the observation, based on published models of the P2Y<sub>2</sub> and P2Y<sub>4</sub> receptors,<sup>8,10,20</sup> that there might have been some space available for the expansion of the ligands around that position. This process led to the synthesis of the first P2Y<sub>4</sub>-selective compounds. In particular, while N<sup>4</sup>-(methyl)-CTP (**11**) was unselective for the two subtypes, N<sup>4</sup>-(phenylpropoxy)-CTP (**16**) and N<sup>4</sup>-(phenylethoxy)-CTP (**15**) were selective for the P2Y<sub>4</sub> receptor with EC<sub>50</sub> values of 23 and 73 nM, respectively. The activity of these CTP analogues contrasts with the weak interaction of CTP itself at the P2Y<sub>2</sub> and

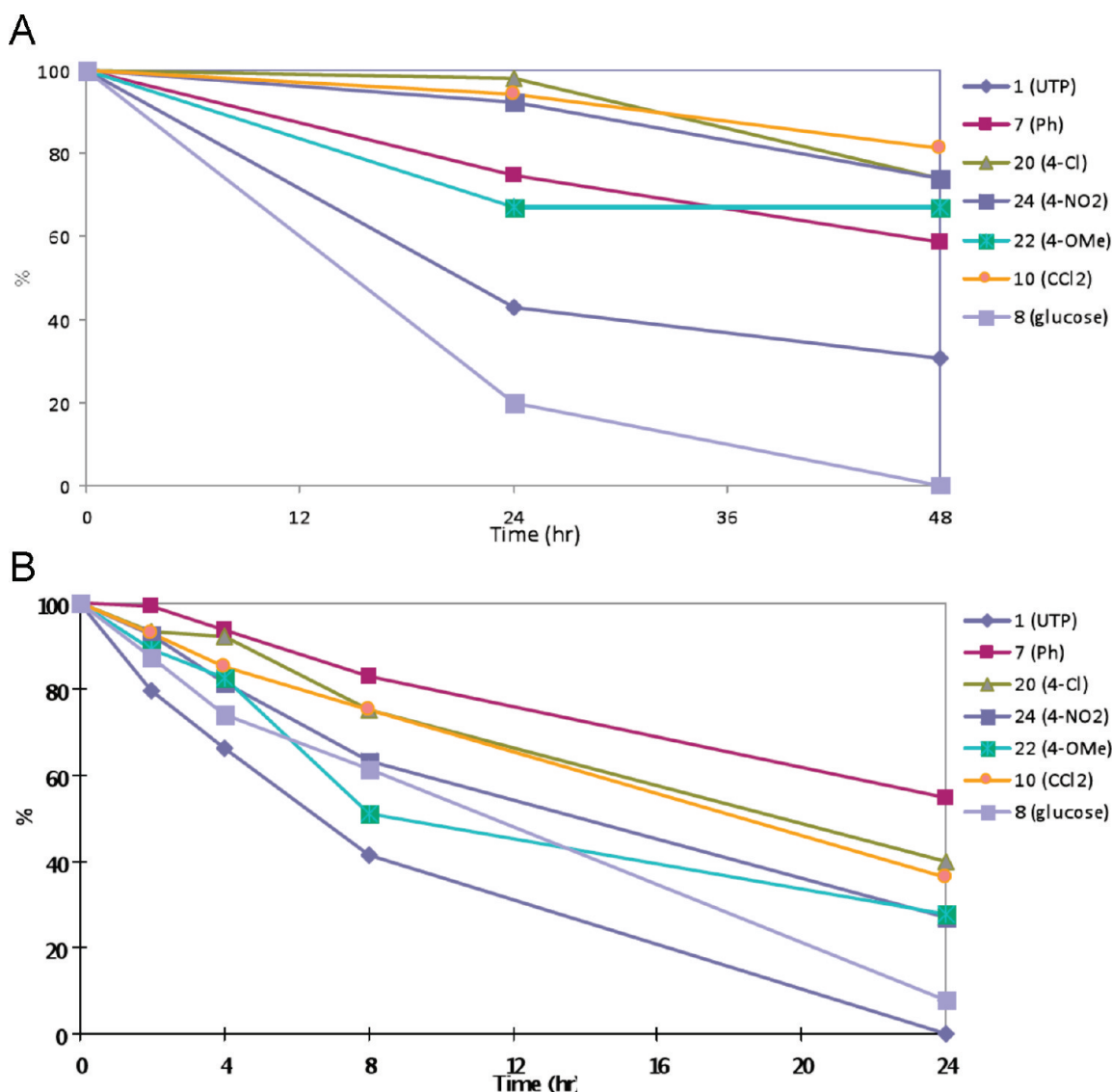


**Figure 7.** (A) Time course of the hydrolysis of various nucleotides incubated at 37 °C and pH 1.5. The assays were started with 0.2 mg/mL of the compound. The concentration of analogues in the medium was determined using HPLC analysis of aliquots. Data are expressed as a percent of the initial peak. (B) Time course of the degradation of various nucleotides in the presence of membranes of 1321N1 astrocytoma cells. The cells were homogenized, and the nuclear fraction was removed by centrifugation. The resultant pellets were suspended in Tris buffer (pH 7.4). The membrane was diluted with Dulbecco's PBS (pH 7.4) and homogenized before use for the stability check. The final protein concentration was 14.9  $\mu\text{g}/\text{mL}$ . The assays were started with 0.2 mg/mL compound. Concentrations of molecules were analyzed using HPLC. Data are expressed as a percent of initial peak.

P2Y<sub>4</sub> receptors.<sup>8</sup> Because our rhodopsin-based models could not explain the different selectivity profiles of the alkoxyimino derivatives, we reconstructed molecular models of the P2Y<sub>2</sub> and P2Y<sub>4</sub> receptors based on the recently disclosed structure of the CXCR4 receptor (Figure 5).<sup>16</sup> The new models incorporate all of the experimentally supported features of the old ones but show a binding mode in which the ligands are slightly shifted toward the extracellular side (Figure 6), which makes them compatible with the new data. In particular, the large substituent of compound 16 protrudes toward EL2, fitting into a cavity substantially larger in the P2Y<sub>4</sub> receptor than in the P2Y<sub>2</sub> receptor, due to the nonconservation of two specific residues. This hypothesis is in good agreement with the selectivity for the P2Y<sub>4</sub> receptor shown by compound 16.

Moreover, by carefully probing substitution of Up<sub>4</sub>-[1]glucose, we identified Up<sub>4</sub>-[1]3'-deoxy-3'-fluoroglucose (34) as modestly

P2Y<sub>4</sub> selective (EC<sub>50</sub> value = 62 nM). However, neither  $\delta$ -phenyl esters nor methylenephosphonates were useful for achieving selectivity for the P2Y<sub>4</sub> receptor. Up<sub>4</sub>- $\delta$ -3-chlorophenyl ester 21 was inactive at P2Y<sub>4</sub> receptors and displayed an EC<sub>50</sub> value at the P2Y<sub>2</sub> receptor of 0.84  $\mu\text{M}$ . The chemical and enzymatic stability of selected derivatives in this series was examined by HPLC to indicate greatly enhanced stability of the  $\delta$ -phenyl phosphoesters but not the  $\delta$ -glucose phosphoesters in comparison to 1. Thus, additional SAR studies will be needed to enhance the stability of P2Y<sub>4</sub> receptor selective agonists. In particular, these studies suggest that the potency, selectivity, and stability of extended uridine tetraphosphate derivatives may be modulated by distal structural changes. N<sup>4</sup>-Alkoxyimino analogues were analyzed in a molecular model, which indicated greater steric tolerance of the N<sup>4</sup>-phenylpropoxy group in the P2Y<sub>4</sub> receptor.

In conclusion, we have synthesized novel uracil nucleotide derivatives that are directed toward selective activation of the P2Y<sub>4</sub> receptor. A series of homologous alkoxyimino derivatives provided an entry to novel selectivity at this subtype. Several of these compounds should be suitable for use as pharmacological probes of the physiological roles of the P2Y<sub>4</sub> receptor.

## EXPERIMENTAL SECTION

**Chemical Synthesis.** <sup>1</sup>H NMR spectra were obtained with a Varian Gemini 300 or Varian Mercury 400 spectrometers using D<sub>2</sub>O, CDCl<sub>3</sub>, or DMSO-*d*<sub>6</sub> as a solvent. The chemical shifts are expressed as relative ppm from HOD (4.80 ppm). <sup>31</sup>P NMR spectra were recorded at room temperature by use of Varian XL 300 (121.42 MHz) or Varian Mercury 400 (162.10 MHz) spectrometers; orthophosphoric acid (85%) was used as an external standard. In several cases, the signal of the terminal phosphate moiety was not visible due to high dilution.

The purity of final nucleotide derivatives was checked using a Hewlett Packard 1100 HPLC equipped with a Zorbax SB-Aq 5 μm analytical column (50 mm × 4.6 mm; Agilent Technologies Inc., Palo Alto, CA). Mobile phase: linear gradient solvent system: 5 mM TBAP (tetrabutylammonium dihydrogenphosphate)–CH<sub>3</sub>CN from 80:20 to 40:60 in 13 min; the flow rate was 0.5 mL/min. Peaks were detected by UV absorption with a diode array detector at 254, 275, and 280 nm. All derivatives tested for biological activity showed >97% purity by HPLC analysis (detection at 254 nm).

High-resolution mass measurements were performed on Micromass/Waters LCT Premier electrospray time of flight (TOF) mass spectrometer coupled with a Waters HPLC system, unless noted. Purification of the nucleotide analogues for biological testing was carried out on (diethylamino)ethyl (DEAE)-A25 Sephadex columns with a linear gradient (0.01–0.5 M) of 0.5 M ammonium bicarbonate as the mobile phase. Compound **10** was purified by Sephadex alone (and isolated in the ammonium salt form), and compounds **11–16** were additionally purified by HPLC with a Luna 5 μm RP-C18(2) semipreparative column (250 mm × 10.0 mm; Phenomenex, Torrance, CA) and using the following conditions: flow rate of 2 mL/min; 10 mM triethylammonium acetate (TEAA)–CH<sub>3</sub>CN from 100:0 to 95:5 (system A) [or up to 99:1 to 50:50 (system B)] in 30 min (and isolated in the triethylammonium salt form). All other compounds were purified only by HPLC. All other reagents were of analytical grade and were purchased from Sigma-Aldrich (St. Louis, MO).

**Uridine-5'-β,γ-dichloromethylene Triphosphate Ammonium Salt (10).** Uridine monophosphate sodium salt (300 mg, 0.93 mmol) and the dichloromethylenediphosphonic acid disodium salt (1 g, 3.46 mmol) were converted to the tributylammonium salts by treatment with ion-exchange resin [DOWEX 50WX2-200 (H)] and tri-*n*-butylamine. After the water was removed, the obtained tributylammonium salts were dried under high vacuum for 1 h. DIC (76.20 μL, 0.90 mmol) was added to a solution of uridine monophosphate tributylammonium salt (0.93 mmol) in *N,N*-dimethylformamide (DMF) (3 mL). After the reaction mixture was stirred at room temperature for 3 h, a solution of dichloromethylenediphosphonic acid tributylammonium salt (3.46 mmol) and MgCl<sub>2</sub> (171.4 mg, 1.8 mmol) in DMF (2 mL) was added. The reaction mixture was stirred at room temperature overnight. After the solvent was removed, the MgCl<sub>2</sub> was removed by treatment with ion-exchange resin [DOWEX 50WX2-200 (H)] and ammonia bicarbonate, and the product **10** was purified by ion-exchange column chromatography with a Sephadex-DEAE A-25 resin. <sup>1</sup>H NMR (D<sub>2</sub>O): δ 7.96 (d, *J* = 7.8 Hz, 1H), 5.96 (m, 2H), 4.43 (m, 1H), 4.37 (m, 1H), 4.36 (m, 2H). <sup>31</sup>P NMR (D<sub>2</sub>O): δ -7.77 (d, *J* = 18.3 Hz), -10.54 (s), -10.79 (s). HRMS-EI found, 548.9043 (M - H)<sup>+</sup>. C<sub>10</sub>H<sub>14</sub>Cl<sub>2</sub>N<sub>2</sub>O<sub>14</sub>P<sub>3</sub> requires

548.9035. HPLC RT 9.7 min (99%) in solvent system A, 1.1 min (98%) in system B.

**General Procedure for the Preparation of Nucleoside Triphosphates (11–16).** A solution of the nucleoside **39–44**<sup>15</sup> (0.073 mmol) and Proton Sponge (24 mg, 0.11 mmol) in trimethyl phosphate (0.4 mL) was stirred for 10 min at 0 °C. Then, phosphorus oxychloride (0.013 mL, 0.13 mmol) was added dropwise, and the reaction mixture was stirred for 2 h at 0 °C. A solution of tributylammonium pyrophosphate (0.8 mL, 0.44 mmol) and tri-*n*-butylamine (0.069 mL, 0.29 mmol) in DMF (1 mL) was added, and stirring was continued at 0 °C for additional 10 min. A 0.2 M concentration of triethylammonium bicarbonate solution (1.5 mL) was added, and the clear solution was stirred at room temperature for 1 h. After solvents were removed, the residue was purified by Sephadex-DEAE A-25 resin and preparative HPLC.

**N<sup>4</sup>-Methoxycytidine-5'-triphosphate Triethylammonium Salt (11).** Compound **11** (37.6 mg, 100%) was obtained as a white solid using N<sup>4</sup>-methoxycytidine **39** (20 mg, 0.073 mmol). <sup>1</sup>H NMR (D<sub>2</sub>O): δ 7.26 (d, *J* = 8.2 Hz, 1H), 5.96 (d, *J* = 6.4 Hz, 1H), 5.82 (d, *J* = 8.2 Hz, 1H), 4.46–4.41 (m, 1H), 4.41–4.37 (m, 1H), 4.28–4.15 (m, 3H), 3.80 (s, 3H). <sup>31</sup>P NMR (D<sub>2</sub>O): δ -11.39 (br), -22.90 (br). HRMS-EI found, 511.9873 (M - H)<sup>+</sup>. C<sub>10</sub>H<sub>17</sub>N<sub>3</sub>O<sub>13</sub>P<sub>3</sub> requires 511.9857; purity >98% by HPLC (system B: 9.08 min).

**N<sup>4</sup>-Ethoxycytidine-5'-triphosphate Triethylammonium Salt (12).** Compound **12** (21.3 mg, 58%) was obtained as a white solid using N<sup>4</sup>-ethoxycytidine **40** (20 mg, 0.070 mmol). <sup>1</sup>H NMR (D<sub>2</sub>O): δ 7.26 (d, *J* = 7.8 Hz, 1H), 5.96 (d, *J* = 6.6 Hz, 1H), 5.82 (d, *J* = 7.8 Hz, 1H), 4.47–4.42 (m, 1H), 4.41–4.34 (m, 1H), 4.28–4.22 (m, 2H), 4.21–4.13 (m, 1H), 4.05 (dd, *J* = 14.2, 7.1 Hz, 2H). <sup>31</sup>P NMR (D<sub>2</sub>O): δ -11.29 (br), -22.10 (br). HRMS-EI found, 526.0029 (M - H)<sup>+</sup>. C<sub>11</sub>H<sub>19</sub>N<sub>3</sub>O<sub>15</sub>P<sub>3</sub> requires 526.0029; purity >98% by HPLC (system B: 10.6 min).

**N<sup>4</sup>-*t*-Butyloxycytidine-5'-triphosphate Triethylammonium Salt (13).** Compound **13** (7.6 mg, 22%) was obtained as a white solid using N<sup>4</sup>-*t*-butyloxycytidine **41** (20 mg, 0.063 mmol). <sup>1</sup>H NMR (D<sub>2</sub>O): δ 7.24 (d, *J* = 8.2 Hz, 1H), 5.97 (d, *J* = 6.4 Hz, 1H), 5.87 (d, *J* = 8.2 Hz, 1H), 4.43–4.35 (m, 2H), 4.26–4.12 (m, 3H), 1.31 (s, 9H). <sup>31</sup>P NMR (D<sub>2</sub>O): δ -9.85 (br), -11.36 (br), -22.99 (br). HRMS-EI found, 554.0342 (M - H)<sup>+</sup>. C<sub>13</sub>H<sub>23</sub>N<sub>3</sub>O<sub>15</sub>P<sub>3</sub> requires 554.0341; purity >98% by HPLC (system B: 9.59 min).

**N<sup>4</sup>-Benzoyloxycytidine-5'-triphosphate Triethylammonium Salt (14).** Compound **14** (16.7 mg, 49%) was obtained as a white solid using N<sup>4</sup>-benzoyloxycytidine **42** (20 mg, 0.057 mmol). <sup>1</sup>H NMR (D<sub>2</sub>O): δ 7.46–7.35 (m, 5H), 7.22 (d, *J* = 8.4 Hz, 1H), 5.95 (d, *J* = 6.5 Hz, 1H), 5.76 (d, *J* = 8.4 Hz, 1H), 5.05 (s, 2H), 4.43–4.32 (m, 2H), 4.26–4.13 (m, 3H). <sup>31</sup>P NMR (D<sub>2</sub>O): δ -10.18 (br), -11.56 (d, *J* = 14.6 Hz), -23.21 (t, *J* = 15.0 Hz). HRMS-EI found, 588.0186 (M - H)<sup>+</sup>. C<sub>16</sub>H<sub>21</sub>N<sub>3</sub>O<sub>15</sub>P<sub>3</sub> requires 588.0200; purity >98% by HPLC (system B: 10.14 min).

**N<sup>4</sup>-Phenylethoxycytidine-5'-triphosphate Triethylammonium Salt (15).** Compound **15** (1.29 mg, 5.5%) was obtained as a white solid using N<sup>4</sup>-(2-phenylethoxy)-cytidine **43** (10 mg, 0.027 mmol). <sup>1</sup>H NMR (D<sub>2</sub>O): δ 7.40–7.29 (m, 5H), 7.23 (d, *J* = 7.6 Hz, 1H), 5.94 (d, *J* = 6.0 Hz, 1H), 5.81 (d, *J* = 8.4 Hz, 1H), 4.43–4.38 (m, 2H), 4.28–4.25 (m, 5H), 3.00 (dd, *J* = 6 Hz, *J* = 6.4 Hz). HRMS-EI found, 602.0342 (M - H)<sup>+</sup>. C<sub>17</sub>H<sub>23</sub>N<sub>3</sub>O<sub>15</sub>P<sub>3</sub> requires 602.0318; purity >98% by HPLC.

**N<sup>4</sup>-Phenylpropoxycytidine-5'-triphosphate Triethylammonium Salt (16).** Compound **16** (0.83 mg, 11%) was obtained as a white solid using N<sup>4</sup>-(3-phenylpropoxy)-cytidine **44** (5 mg, 0.013 mmol). <sup>1</sup>H NMR (D<sub>2</sub>O): δ 7.38–7.31 (m, 5H), 7.23 (d, *J* = 8.4 Hz, 1H), 5.95 (d, *J* = 6.0 Hz, 1H), 5.78 (d, *J* = 8.4 Hz, 1H), 4.42–4.38 (m, 2H), 4.25–4.23 (m, 3H), 4.06 (dd, *J* = 5.5 Hz, *J* = 6.1 Hz, 2H), 2.75 (dd, *J* = 7.28 Hz, *J* = 7.45 Hz, 2H), 4.20 (m, 2H). <sup>31</sup>P NMR (D<sub>2</sub>O): δ -5.51 (m), -10.34 (m), -10.81 (m). HRMS-EI found, 616.0486 (M - H)<sup>+</sup>. C<sub>18</sub>H<sub>25</sub>N<sub>3</sub>O<sub>15</sub>P<sub>3</sub> requires 616.0496; purity >98% by HPLC.

**General Procedure for the Preparation of Nucleoside Tetrphosphate Phenyl Derivatives (20–25).** The corresponding aryl monophosphate<sup>15</sup> (0.036 mmol) and **1** as a trisodium salt (10 mg, 0.018 mmol) were converted to the tributylammonium salts by treatment with ion-exchange resin [DOWEX 50WX2-200 (H)] and tri-*n*-butylamine. After the water was removed, the obtained tributylammonium salts were dried under high vacuum for 1 h. DIC (3.05  $\mu$ L, 0.036 mmol) was added to a solution of uridine triphosphate tributylammonium salt (0.018 mmol) in DMF (0.2 mL). After the reaction mixture was stirred at room temperature for 1 h, a solution of the corresponding aryl monophosphate tributylammonium salt (0.036 mmol) and MgCl<sub>2</sub> (3.43 mg, 0.036 mmol) in DMF (0.1 mL) was added. The reaction mixture was stirred at room temperature overnight. After the solvent was removed, the MgCl<sub>2</sub> was removed by treatment with ion-exchange resin [DOWEX 50WX2-200 (H)] and ammonia bicarbonate or tri-*n*-butylamine, and the residue was purified by a semipreparative HPLC.

**Uridine-5'-(4-chlorophenyl)-tetrphosphate Triethylammonium Salt (20).** Compound **20** (0.3 mg, 6%) was obtained as a white solid using **1** (12 mg, 0.022 mmol). <sup>1</sup>H NMR (D<sub>2</sub>O):  $\delta$  7.93 (d, *J* = 7.5 Hz, 1H), 7.38 (d, *J* = 8.4 Hz, 2H), 7.25 (d, *J* = 8.4 Hz, 2H), 5.97 (d, *J* = 5.4 Hz, 1H), 5.93 (d, *J* = 7.8 Hz, 1H), 4.42–4.30 (m, 2H), 4.27–4.21 (m, 3H). <sup>31</sup>P NMR (D<sub>2</sub>O):  $\delta$  -11.20 (br), -15.74 (br), -23.04 (br). HRMS-EI found, 672.9218 (M - H<sup>+</sup>)<sup>-</sup>. C<sub>15</sub>H<sub>18</sub>N<sub>2</sub>O<sub>18</sub>P<sub>4</sub>Cl requires 672.9194; purity >98% by HPLC (system B: 11.9 min).

**Uridine-5'-(3-chlorophenyl)-tetrphosphate Triethylammonium Salt (21).** Compound **21** (1.4 mg, 12%) was obtained as a white solid using **1** (10 mg, 0.018 mmol). <sup>1</sup>H NMR (D<sub>2</sub>O):  $\delta$  7.88 (d, *J* = 8.1 Hz, 1H), 7.36–7.12 (m, 4H), 5.91 (d, *J* = 5.1 Hz, 1H), 5.79 (d, *J* = 8.1 Hz, 1H), 4.39–4.28 (m, 2H), 4.23–4.17 (m, 3H). <sup>31</sup>P NMR (D<sub>2</sub>O):  $\delta$  -11.20 (d, *J* = 18.3 Hz), -15.84 (d, *J* = 17.5 Hz), -23.14 (m). HRMS-EI found, 672.9218 (M - H<sup>+</sup>)<sup>-</sup>. C<sub>15</sub>H<sub>18</sub>N<sub>2</sub>O<sub>18</sub>P<sub>4</sub>Cl requires 672.9194; purity >98% by HPLC (system B: 12.2 min).

**Uridine-5'-(4-methoxyphenyl)-tetrphosphate Triethylammonium Salt (22).** Compound **22** (2.7 mg, 22%) was obtained as a white solid using **1** (10 mg, 0.018 mmol). <sup>1</sup>H NMR (D<sub>2</sub>O):  $\delta$  7.88 (d, *J* = 8.4 Hz, 1H), 7.17 (d, *J* = 9.0 Hz, 2H), 6.92 (d, *J* = 9.0 Hz, 2H), 5.91 (d, *J* = 5.1 Hz, 1H), 5.88 (d, *J* = 8.4 Hz, 1H), 4.37–4.25 (m, 2H), 4.23–4.16 (m, 3H), 3.78 (s, 3H). <sup>31</sup>P NMR (D<sub>2</sub>O):  $\delta$  -11.19 (br, 1H), -15.04 (br, 1H), -23.00 (br, 2H). HRMS-EI found, 668.9681 (M - H<sup>+</sup>)<sup>-</sup>. C<sub>16</sub>H<sub>21</sub>N<sub>2</sub>O<sub>19</sub>P<sub>4</sub> requires 668.9689; purity >98% by HPLC (system A: 12.1 min).

**Uridine-5'-(3-methoxyphenyl)-tetrphosphate Triethylammonium Salt (23).** Compound **23** (1.9 mg, 16%) was obtained as a white solid using **1** (10 mg, 0.018 mmol). <sup>1</sup>H NMR (D<sub>2</sub>O):  $\delta$  7.89 (d, *J* = 8.1 Hz, 1H), 7.26 (t, *J* = 8.1 Hz, 1H), 6.90–6.82 (m, 2H), 6.72 (d, *J* = 8.1 Hz, 1H), 5.91 (d, *J* = 6.0 Hz, 1H), 5.88 (d, *J* = 8.7 Hz, 1H), 4.38–4.24 (m, 2H), 4.22–4.16 (m, 3H), 3.80 (s, 3H). <sup>31</sup>P NMR (D<sub>2</sub>O):  $\delta$  -11.20 (d, *J* = 18.4 Hz, 1H), -15.69 (d, *J* = 17.5 Hz, 1H), -23.14 (m, 2H). HRMS-EI found, 668.9699 (M - H<sup>+</sup>)<sup>-</sup>. C<sub>16</sub>H<sub>21</sub>N<sub>2</sub>O<sub>19</sub>P<sub>4</sub> requires 668.9689; purity >98% by HPLC (system A: 12.1 min).

**Uridine-5'-(4-nitrophenyl)-tetrphosphate Triethylammonium Salt (24).** Compound **24** (2.2 mg, 23%) was obtained as a white solid using **1** (12 mg, 0.022 mmol). <sup>1</sup>H NMR (D<sub>2</sub>O):  $\delta$  8.23 (d, *J* = 8.7 Hz, 2H), 7.87 (d, *J* = 8.4 Hz, 1H), 7.41 (d, *J* = 8.7 Hz, 2H), 5.91 (d, *J* = 5.1 Hz, 1H), 5.87 (d, *J* = 8.4 Hz, 1H), 4.37–4.28 (m, 2H), 4.22–4.17 (m, 3H). <sup>31</sup>P NMR (D<sub>2</sub>O):  $\delta$  -11.14 (d, *J* = 17.5 Hz, 1H), -16.83 (d, *J* = 16.9 Hz, 1H), -23.06 (m, 2H). HRMS-EI found, 683.9434 (M - H<sup>+</sup>)<sup>-</sup>. C<sub>15</sub>H<sub>18</sub>N<sub>3</sub>O<sub>20</sub>P<sub>4</sub> requires 683.9434; purity >98% by HPLC (system A: 11.6 min).

**Uridine-5'-(3-nitrophenyl)-tetrphosphate Triethylammonium Salt (25).** Compound **25** (3.4 mg, 41%) was obtained as a white solid using **1** (10 mg, 0.018 mmol). <sup>1</sup>H NMR (D<sub>2</sub>O):  $\delta$  8.27 (d, *J* = 12.0 Hz, 2H), 7.92 (d, *J* = 8.1 Hz, 1H), 7.44 (d, *J* = 12.0 Hz, 2H), 5.96–5.88

(m, 2H), 4.41–4.30 (m, 2H), 4.25–4.19 (m, 3H). <sup>31</sup>P NMR (D<sub>2</sub>O):  $\delta$  -11.18 (d, *J* = 14.5 Hz), -16.89 (d, *J* = 14.5 Hz), -22.80–23.60 (m). HRMS-EI found, 683.9434 (M - H<sup>+</sup>)<sup>-</sup>. C<sub>15</sub>H<sub>18</sub>N<sub>3</sub>O<sub>20</sub>P<sub>4</sub> requires 683.9438; purity >98% by HPLC (system A: 13.1 min).

**Uridine-5'-glucose-1'- $\beta$ , $\gamma$ -dichloromethylene Tetrphosphate Triethylammonium Salt (26).** Compound **10** (3.4 mg, 0.006 mmol) and glucose-1-phosphate disodium salt hydrate (4 mg, 0.036 mmol) were converted to the tributylammonium salts by treatment with ion-exchange resin [DOWEX 50WX2-200 (H)] and tri-*n*-butylamine. After the water was removed, the obtained tributylammonium salts were dried under high vacuum for 1 h. DIC (3.05  $\mu$ L, 0.036 mmol) was added to a solution of **10** (0.006 mmol) in DMF (0.2 mL). After the reaction mixture was stirred at room temperature for 1 h, a solution of glucose-1-phosphate tributylammonium salt (0.036 mmol) and MgCl<sub>2</sub> (3.43 mg, 0.036 mmol) in DMF (0.1 mL) was added. The reaction mixture was stirred at room temperature overnight. After the solvent was removed, the MgCl<sub>2</sub> was removed by treatment with ion-exchange resin [DOWEX 50WX2-200 (H)] and ammonia bicarbonate or tri-*n*-butylamine, and the residue was purified by a semipreparative HPLC to obtain **26** (0.32 mg, 7%) as a white solid. <sup>1</sup>H NMR (D<sub>2</sub>O):  $\delta$  8.02 (d, *J* = 8.1 Hz, 1H), 6.04–5.97 (m, 2H), 5.71–5.67 (m, 1H), 4.53–4.47 (m, 1H), 4.44–4.38 (m, 1H), 4.37–4.25 (m, 3H), 4.00–3.73 (m, 4H), 3.57–3.41 (m, 2H). <sup>31</sup>P NMR (D<sub>2</sub>O):  $\delta$  8.08 (d, *J* = 19.1 Hz), 1.90–0.02 (br), -10.48 (s), -10.74 (s). HRMS-EI found, 790.9233 (M - H<sup>+</sup>)<sup>-</sup>. C<sub>16</sub>H<sub>26</sub>N<sub>2</sub>O<sub>22</sub>P<sub>4</sub>Cl requires 790.9227; purity >98% by HPLC (system A: 10.3 min).

**General Procedure for the Preparation of Nucleoside Tetrphosphate Sugars (28–37).** The appropriate sugar **63–67** was treated with a mixture of sodium acetate (50 mg) in acetic anhydride (5 mL), and the mixture was stirred for 5 h at 110 °C while following the course of the reaction by TLC. Excess Ac<sub>2</sub>O was removed using a rotary evaporator, and the mixture was stirred with aqueous NaHCO<sub>3</sub> for 15 min. The product was extracted into dichloromethane and washed with brine. The corresponding crude acetyl derivative was purified by column chromatography. The monophosphate derivatives (**68–72**) of these acetyl sugars were prepared as the lithium salts using the MacDonald procedure.<sup>39</sup> The corresponding sugar monophosphate (0.036 mmol) and uridine triphosphate trisodium salt (10 mg, 0.018 mmol) were converted to the tributylammonium salts by treatment with ion-exchange resin [DOWEX 50WX2-200 (H)] and tri-*n*-butylamine. After the water was removed, the obtained tributylammonium salts were dried under high vacuum for 1 h. DIC (3.05  $\mu$ L, 0.036 mmol) was added to a solution of **1** as a tributylammonium salt (0.018 mmol) in DMF (0.2 mL). After the reaction mixture was stirred at room temperature for 3 h, a solution of the corresponding sugar monophosphate tributylammonium salt (0.036 mmol) and MgCl<sub>2</sub> (3.43 mg, 0.036 mmol) in DMF (0.1 mL) was added. The reaction mixture was stirred at room temperature for 2 h to overnight. After the solvent was removed, the MgCl<sub>2</sub> was removed by treatment with ion-exchange resin [DOWEX 50WX2-200 (H)] and ammonia bicarbonate or tri-*n*-butylamine, and the residue was purified by a semipreparative HPLC purification using system C.

**Uridine-5'-allose-1'-tetrphosphate Triethylammonium Salt (28).** Compound **28** (1 mg, 8%) was obtained as a white solid using **1** (10 mg, 0.018 mmol) and D-allose-1-phosphate (**69**, 16.5 mg, 0.036 mmol). <sup>1</sup>H NMR (D<sub>2</sub>O):  $\delta$  7.95 (d, *J* = 8.1 Hz, 1H), 5.98 (m, 2H), 5.60 (m, 1H), 4.16 (m, 2H), 4.33 (m, 1H), 4.28–4.23 (m, 2H), 3.90–3.60 (m, 4H), 3.54 (m, 1H), 3.41 (m, 1H). <sup>31</sup>P NMR (D<sub>2</sub>O):  $\delta$  -11.29 (m), -12.40 (m), -22.86 (m). HRMS-EI found, 724.9831 (M - H<sup>+</sup>)<sup>-</sup>. C<sub>15</sub>H<sub>25</sub>N<sub>2</sub>O<sub>23</sub>P<sub>4</sub> requires 724.9804. HPLC (purity 97%, system A: 11.5 min; purity 98%, system B: 0.8 min).

**Uridine-5'-mannose-1'-tetrphosphate Triethylammonium Salt (29).** Compound **29** (3.18 mg, 24%) was obtained as a white solid using **1** (10 mg, 0.018 mmol) and D-mannose-1-phosphate (**68**, 16.5 mg, 0.036 mmol). <sup>1</sup>H NMR (D<sub>2</sub>O):  $\delta$  7.99 (d, *J* = 8.4 Hz, 1H),

6.02 (m, 2H), 5.56 (m, 1H), 4.44 (m, 2H), 4.31–4.27 (m, 3H), 4.16 (m, 1H), 4.03–3.87 (m, 3H), 3.79 (m, 1H), 3.67 (m, 1H).  $^{31}\text{P}$  NMR ( $\text{D}_2\text{O}$ ):  $\delta$  –11.17 (d,  $J$  = 17.6 Hz), –12.63 (d,  $J$  = 17.5 Hz), –23.10 (m). HRMS-EI found, 724.9796 ( $\text{M} - \text{H}$ ) $^+$ .  $\text{C}_{15}\text{H}_{25}\text{N}_2\text{O}_{23}\text{P}_4$  requires 724.9799. HPLC (purity 99%, system A: 10.4 min; purity 99%, system B: 1.1 min).

**Uridine-5'-xylose-1'-tetraphosphate Triethylammonium Salt (30).** Compound 30 (3.18 mg, 43%) was obtained as a white solid using **1** (6.3 mg, 0.011 mmol) and D-xylose-1-phosphate (14 mg, 0.032 mmol).  $^1\text{H}$  NMR ( $\text{D}_2\text{O}$ ):  $\delta$  8.00 (d,  $J$  = 8.4 Hz, 1H), 6.07–5.98 (m, 2H), 5.64–5.58 (m, 1H), 4.50–4.40 (m, 2H), 4.36–4.23 (m, 3H), 3.83–3.76 (m, 1H), 3.69–3.60 (m, 1H), 3.58–3.49 (m, 1H), 3.47–3.37 (m, 1H).  $^{31}\text{P}$  NMR ( $\text{D}_2\text{O}$ ):  $\delta$  –11.22 (d,  $J$  = 16.8 Hz), –12.65 (d,  $J$  = 18.2 Hz), –22.6 to –23.4 (m). HRMS-EI found, 694.9693 ( $\text{M} - \text{H}$ ) $^-$ .  $\text{C}_{14}\text{H}_{23}\text{N}_2\text{O}_{22}\text{P}_4$  requires 694.9656; purity >98% by HPLC (system B: 12.3 min).

**General Procedure for the Preparation of Nucleoside Tetraphosphate Sugars (31 and 32).** The corresponding sodium salt of sugar monophosphate (0.036 mmol) and the trisodium salt of **1** (10 mg, 0.018 mmol) were converted to the tributylammonium salts by treatment with ion-exchange resin [DOWEX 50WX2-200 (H)] and tri-*n*-butylamine. After the water was removed, the obtained tributylammonium salts were dried under high vacuum 1 h. DIC (3.05  $\mu\text{L}$ , 0.036 mmol) was added to a solution of **1** as a tributylammonium salt (0.018 mmol) in DMF (0.2 mL). After the reaction mixture was stirred at room temperature for 3 h, a solution of the corresponding sugar monophosphate tributylammonium salt (0.036 mmol) and  $\text{MgCl}_2$  (3.43 mg, 0.036 mmol) in DMF (0.1 mL) was added. The reaction mixture was stirred at room temperature for 2 h to overnight. After the solvent was removed, the  $\text{MgCl}_2$  was removed by treatment with ion-exchange resin [DOWEX 50WX2-200 (H)] and ammonia bicarbonate or tri-*n*-butylamine, and the residue was purified by a semipreparative HPLC purification using system C.

**$\text{P}^1$ -(Uridine-5')- $\text{P}^4$ -(2'-deoxy-2'-acetamidoglucose-1')-tetraphosphate Triethylammonium Salt (31).** Compound 31 (5.21 mg, 38%) was obtained as a white solid using **1** (10 mg, 0.018 mmol) and D-2-deoxy-2-acetamidoglucose-1-phosphate (12.5 mg, 0.036 mmol).  $^1\text{H}$  NMR ( $\text{D}_2\text{O}$ ):  $\delta$  7.99 (d,  $J$  = 8.1 Hz, 1H), 6.02 (m, 2H), 5.53 (m, 1H), 4.44 (m, 2H), 4.29 (m, 3H), 4.02–3.80 (m, 4H), 3.53 (m, 1H), 2.11 (s, 3H), 1.93 (s, 1H).  $^{31}\text{P}$  NMR ( $\text{D}_2\text{O}$ ):  $\delta$  –11.17 (d,  $J$  = 18.3 Hz), –12.77 (d,  $J$  = 19.0 Hz), –23.10 (m). HRMS-EI found, 766.0037 ( $\text{M} - \text{H}$ ) $^+$ .  $\text{C}_{17}\text{H}_{28}\text{N}_3\text{O}_{23}\text{P}_4$  requires 766.0064. HPLC (purity 99%, system A: 10.4 min; purity 99%, system B: 0.8 min).

**$\text{P}^1$ -(Uridine-5')- $\text{P}^4$ -(glucuronic acid-1')-tetraphosphate Triethylammonium Salt (32).** Compound 32 (2.46 mg, 18%) was obtained as a white solid using **1** (10 mg, 0.018 mmol) and  $\alpha$ -D-glucuronic acid 1-phosphate (**74**, 12.2 mg, 0.036 mmol).  $^1\text{H}$  NMR ( $\text{D}_2\text{O}$ ):  $\delta$  7.95 (d,  $J$  = 7.5 Hz, 1H), 5.99 (m, 2H), 5.65 (m, 1H), 4.39 (m, 2H), 4.27–4.23 (m, 3H), 4.10 (m, 1H), 3.80 (m, 1H), 3.51 (s, 2H).  $^{31}\text{P}$  NMR ( $\text{D}_2\text{O}$ ):  $\delta$  –11.18 (d,  $J$  = 17.6 Hz), –12.55 (d,  $J$  = 16.7 Hz), –22.71 (m). HRMS-EI found, 738.9575 ( $\text{M} - \text{H}$ ) $^+$ .  $\text{C}_{17.5}\text{H}_{23}\text{N}_2\text{O}_{24}\text{P}_4$  requires 738.9591. HPLC (purity 97%, system A: 11.4 min; purity 99%, system B: 1.0 min).

**$\text{P}^1$ -(Uridine-5')- $\text{P}^4$ -(2'-deoxy-2'-fluoroglucose-1')-tetraphosphate Triethylammonium Salt (33).** Compound 33 (3.28 mg, 25%) was obtained as a white solid using **1** (10 mg, 0.018 mmol) and D-2-deoxy-2-fluoroglucose-1-phosphate (**70**, 16.57 mg, 0.036 mmol).  $^1\text{H}$  NMR ( $\text{D}_2\text{O}$ ):  $\delta$  7.99 (d,  $J$  = 8.1 Hz, 1H), 6.01 (m, 2H), 5.82 (m, 1H), 4.44 (m, 2H), 4.28 (m, 3H), 4.12–3.71 (m, 4H), 3.52 (m, 1H).  $^{31}\text{P}$  NMR ( $\text{D}_2\text{O}$ ):  $\delta$  –11.10 (d,  $J$  = 16.7 Hz), –13.10 (d,  $J$  = 17.5 Hz), –23.07 (m). HRMS-EI found, 726.9753 ( $\text{M} - \text{H}$ ) $^+$ .  $\text{C}_{15}\text{H}_{24}\text{FN}_2\text{O}_{23}\text{P}_4$  requires 726.9761. HPLC (purity 99%, system A: 10.3 min; purity 98%, system B: 1.1 min).

**$\text{P}^1$ -(Uridine-5')- $\text{P}^4$ -(3'-deoxy-3'-fluoroglucose-1')-tetraphosphate Triethylammonium Salt (34).** Compound 34 (3.58 mg, 27%) was obtained as a white solid using **1** (10 mg, 0.018 mmol) and

D-3-deoxy-3-fluoroglucose-1-phosphate (**71**, 16.57 mg, 0.036 mmol).  $^1\text{H}$  NMR ( $\text{D}_2\text{O}$ ):  $\delta$  7.92 (d,  $J$  = 8.1 Hz, 1H), 5.98 (m, 2H), 5.61 (m, 1H), 4.35 (m, 2H), 4.27–4.21 (m, 4H), 3.99–3.72 (m, 3H).  $^{31}\text{P}$  NMR ( $\text{D}_2\text{O}$ ):  $\delta$  –11.08 (m), –12.87 (m), –22.38 (m). HRMS-EI found, 726.9763 ( $\text{M} - \text{H}$ ) $^+$ .  $\text{C}_{15}\text{H}_{24}\text{FN}_2\text{O}_{23}\text{P}_4$  requires 726.9761. HPLC (purity 98%, system A: 10.4 min; purity 98%, system B: 1.0 min).

**$\text{P}^1$ -( $N^4$ -Benzyloxycytidine-5')- $\text{P}^4$ -(3'-deoxy-3'-fluoroglucose-1')-tetraphosphate Triethylammonium Salt (35).** Compound 35 (0.550 mg, 2.6%) was obtained as a white solid using triethylammonium salt of  $N^4$ -benzyloxycytidine 5'-triphosphate (14.45 mg, 0.018 mmol) and D-3-deoxy-3-fluoroglucose-1-phosphate (**71**, 14.76 mg, 0.036 mmol).  $^1\text{H}$  NMR ( $\text{D}_2\text{O}$ ):  $\delta$  7.44 (m, 5H), 7.23 (d,  $J$  = 8.8 Hz, 1H), 5.96 (d,  $J$  = 6.4 Hz, 1H), 5.77 (d,  $J$  = 8.4 Hz, 1H), 5.05 (s, 2H), 4.46–4.42 (m, 2H), 4.38–4.17 (m, 4H), 3.99–3.72 (m, 3H).  $^{31}\text{P}$  NMR ( $\text{D}_2\text{O}$ ):  $\delta$  –11.53 (m), –13.27 (m), –23.21 (m). HRMS-EI found, 832.0319 ( $\text{M} - \text{H}$ ) $^+$ .  $\text{C}_{22}\text{H}_{31}\text{FN}_3\text{O}_{22}\text{P}_4$  requires 726.9761.

**$\text{P}^1$ -( $N^4$ -Methoxycytidine-5')- $\text{P}^4$ -(3'-deoxy-3'-fluoroglucose-1')-tetraphosphate Triethylammonium Salt (36).** Compound 36 (0.80 mg, 8.8%) was obtained as a white solid using triethylammonium salt of  $N^4$ -methoxycytidine 5'-triphosphate (9 mg, 0.012 mmol) and D-3-deoxy-3-fluoroglucose-1-phosphate (**71**, 10 mg, 0.025 mmol).  $^1\text{H}$  NMR ( $\text{D}_2\text{O}$ ):  $\delta$  7.26 (d,  $J$  = 7.6 Hz, 1H), 5.96 (d,  $J$  = 6.92 Hz, 1H), 5.83 (d,  $J$  = 8.2 Hz, 1H), 5.69 (m, 1H), 4.42–4.37 (m, 2H), 4.26–4.15 (m, 4H), 3.99–3.89 (m, 2H), 3.80 (m, 5H). HRMS-EI found, 756.0002 ( $\text{M} - \text{H}$ ) $^+$ .  $\text{C}_{16}\text{H}_{27}\text{FN}_3\text{O}_{24}\text{P}_4$  requires 756.0021; purity 97% by HPLC (system B: 13.5 min).

**$\text{P}^1$ -(Uridine-5')- $\text{P}^4$ -(4'-deoxy-4'-fluoroglucose-1')-tetraphosphate Triethylammonium Salt (37).** Compound 37 (2.88 mg, 22%) was obtained as a white solid using **1** (10 mg, 0.018 mmol) and D-4-deoxy-4-fluoroglucose-1-phosphate (**72**, 16.57 mg, 0.036 mmol).  $^1\text{H}$  NMR ( $\text{D}_2\text{O}$ ):  $\delta$  7.99 (d,  $J$  = 8.1 Hz, 1H), 6.02 (m, 2H), 5.66 (m, 1H), 4.45 (m, 2H), 4.28 (m, 3H), 4.17–4.06 (m, 2H), 3.99–3.77 (m, 2H), 3.60 (m, 1H).  $^{31}\text{P}$  NMR ( $\text{D}_2\text{O}$ ):  $\delta$  –11.12 (d,  $J$  = 17.6 Hz), –12.70 (d,  $J$  = 16.6 Hz), –23.17 (m). HRMS-EI found, 726.9753 ( $\text{M} - \text{H}$ ) $^+$ .  $\text{C}_{15}\text{H}_{24}\text{FN}_2\text{O}_{23}\text{P}_4$  requires 726.9761. HPLC (purity 97%, system A: 11.0 min; purity 99%, system B: 1.1 min).

**$\alpha$ -D-Glucuronic Acid 1-Phosphate Trisodium Salt (74).** TEMPO (10 mg, 64  $\mu\text{mol}$ ) was added to a solution of  $\alpha$ -D-glucose-1-phosphate disodium salt (**73**, 4.13 g, 13.6 mmol) in  $\text{H}_2\text{O}$  (4 mL) at 0  $^\circ\text{C}$ . To this solution, aqueous 1 M NaOH was added until pH 9 was reached, and a NaOCl solution (1.2 mL, available chlorine: 10–13%) was added slowly. The pH was maintained at 9 by adding 1 M NaOH(aq) several times during the reaction. After 1.5 h, MeOH was added to the reaction mixture, and the resulting precipitate was collected by filtration to give **74** (415 mg, 90%) as a white solid.  $^1\text{H}$  NMR ( $\text{D}_2\text{O}$ ):  $\delta$  5.46 (dd, 1H,  $J$  = 3.6, 7.5 Hz), 4.15 (d, 1H,  $J$  = 10.2 Hz), 3.79 (t, 1H,  $J$  = 9.6 Hz), 3.48 (d, 1H,  $J$  = 9.6 Hz), 3.47 (t, 1H,  $J$  = 9.6 Hz). HRMS-ES $^-$  found, 294.9831 ( $\text{M} + \text{Na} - 2\text{H}$ ) $^-$ .  $\text{C}_6\text{H}_9\text{O}_{10}\text{PNa}$  requires 294.9837.

**Assay of PLC Activity Stimulated by P2Y<sub>2</sub>, P2Y<sub>4</sub>, and P2Y<sub>6</sub> Receptors.** Stable cell lines expressing the human P2Y<sub>2</sub>, P2Y<sub>4</sub>, or P2Y<sub>6</sub> receptor in 1321N1 human astrocytoma cells were generated as described.<sup>19</sup> Agonist-induced [ $^3\text{H}$ ]inositol phosphate production was measured in 96-well plates that received 20000 cells/well 2 days prior to assay. Sixteen hours before the assay, the inositol lipid pool of the cells was radiolabeled by incubation in 100  $\mu\text{L}$  of serum-free inositol-free Dulbecco's modified Eagle's medium containing 1.0  $\mu\text{Ci}$  of *myo*-[ $^3\text{H}$ ]inositol. No changes of medium were made subsequent to the addition of [ $^3\text{H}$ ]inositol. On the day of the assay, cells were challenged with 25  $\mu\text{L}$  of a 5-fold concentrated solution of receptor agonists in 200 mM HEPES (*N*-2-hydroxyethylpiperazine-*N'*-2-ethanesulfonic acid), pH 7.3, in Hank's balanced salt solution, containing 50 mM LiCl for 30 min at 37  $^\circ\text{C}$ . Incubations were terminated by aspiration of the drug-containing medium and addition of 450  $\mu\text{L}$  of ice-cold 50 mM formic acid. [ $^3\text{H}$ ]Inositol phosphate

accumulation was quantified using scintillation proximity assay methodology as previously described in detail.<sup>19</sup>

**Data Analysis.** Agonist potencies ( $EC_{50}$  values) were determined from concentration–response curves by nonlinear regression analysis using the GraphPad software package Prism (GraphPad, San Diego, CA). All experiments examining the activity of newly synthesized molecules also included full concentration effect curves for the cognate agonist of the target receptor: **1** for the P2Y<sub>2</sub> and P2Y<sub>4</sub> receptors and UDP for the P2Y<sub>6</sub> receptor. Each concentration of drug was tested in triplicate assays, and concentration effect curves for each test drug were repeated in at least three separate experiments with freshly diluted molecule. The results are presented as means  $\pm$  SEMs from multiple experiments or in the case of concentration effect curves from a single experiment carried out with triplicate assays that were representative of results from multiple experiments.

**Molecular Modeling.** Molecular models of the P2Y<sub>2</sub> and P2Y<sub>4</sub> receptors were constructed with the molecular operating environment (MOE)<sup>40</sup> on the basis of the crystal structure of the CXCR4 chemokine receptor.<sup>16</sup> An initial sequence alignment was obtained with the Blossum62 substitution matrix, with penalties for gap insertions and extensions of 7 and 1, respectively. The proper alignment of the conserved motifs that characterize each of the TM helices was checked and, when necessary, manually adjusted. All of the gaps in the alignment of the TM helices were eliminated; gaps in the loops were consolidated into a single gap per loop and positioned where insertions or deletions seemed compatible with the structure of the template. The final alignment used for the construction of the model is provided in Figure 4. Ten models were built and scored on the basis of electrostatic solvation energy (GB/VI).<sup>41</sup> Intermediate and final models were subjected to energy minimizations with the Amber99 force field, according to the protocol implemented in MOE, with the refinement level set to medium.<sup>40</sup>

As mentioned, a disulfide bridge connects the N-terminus and the extracellular end of TM7 in the CXCR4 receptor and, putatively, in the P2Y receptors, according to mutagenesis data.<sup>22–24</sup> However, as evident from Figure 4, in the P2Y receptors, this cysteine residue is shifted two residues downstream with respect to the CXCR4 receptor. Thus, before the construction of the homology model, the N-terminal region of the template was modified ad hoc. In particular, Cys28 and Arg30 of CXCR4 were mutated to alanine and cysteine, respectively, and a disulfide bridge was built between Cys28 and Cys274. The mutated CXCR4 receptor was then subjected to energy minimization with MOE,<sup>37</sup> with the Amber99 force field, until reaching a cutoff parameter on the potential energy gradient of 0.05 kcal/(mol Å). During the minimization, the two cysteines and all of the N-terminal residues were granted flexibility.

After the construction of the homology models, **1** was docked into the P2Y<sub>2</sub> and P2Y<sub>4</sub> receptors superimposing our previously published complexes to the new models. For each receptor, the ligand was then subjected to two subsequent energy minimizations, the first holding the receptor frozen, the second one granting flexibility to all residues within a 5 Å radius from the ligand. The energy minimizations were conducted in MOE,<sup>40</sup> with the MMFFx force field, until reaching a cutoff parameter on the potential energy gradient of 0.05 kcal/(mol Å). Compounds **11** and **16** were then sketched from **1** within the P2Y<sub>2</sub> and P2Y<sub>4</sub> receptors, respectively, and subsequently subjected to the same two rounds of minimization following the same protocol outlined above for **1**. The obtained P2Y<sub>2</sub>-**11** and P2Y<sub>4</sub>-**16** complexes were subsequently transferred to Maestro<sup>42</sup> and subjected to conformational searches with the MacroModel engine,<sup>43</sup> as implemented in the Schrodinger package. Flexibility was granted to the ligands and the residues within a 5 Å radius from them. All of the atoms within an additional shell of a 3 Å radius were also taken into account as a frozen environment. The calculations were conducted with the MMFFs force field, using water as implicit solvent (GB/SA model).<sup>44</sup> The minimizations were based on the

Polak–Ribiere conjugate gradient algorithm and were performed with a threshold on the potential energy gradient of 0.05 kcal/(mol Å). The conformational searches were based on 100 steps of extended Monte Carlo multiple minimum (MCM) sampling protocol. Specifically, the sampling regarded all torsion angles of residues and ligands as well as ligand rotation and ligand translation.

The interhelical cavities of the P2Y<sub>2</sub> and P2Y<sub>4</sub> receptor were analyzed with the SiteMap program, implemented in the Schrodinger package, cropping site maps at 2 Å from the nearest site point.<sup>44</sup>

**Stability of Nucleotide Derivatives.** Compound **1** was purchased from Sigma (St. Louis, MO). Compound **2** was synthesized by the procedure previously reported.<sup>13</sup> HCl buffer (pH 1.5) solution was prepared as follows. Concentrated HCl (7 mL, 12 N) was added to 2.0 g of sodium chloride and diluted with water to a volume of 1000 mL. Membranes were prepared as follows. P2Y<sub>1</sub> receptor-expressing astrocytoma cells were grown to 80% confluence and then harvested. The cells were homogenized, and the nuclear fraction was removed by centrifugation at 100g for 5 min. The pellet was resuspended in 50 mM tris-(hydroxymethyl)aminomethane (Tris) hydrochloride buffer (pH 7.4). The suspension was homogenized with a polytron homogenizer (Brinkmann) for 10 s and was ultracentrifuged at 20000g for 20 min at 4 °C. The resultant pellets were resuspended in Tris buffer (pH 7.4), and the membrane was stored at –80 °C until the experiments. The protein concentration of the membrane preparation was measured using the Bradford assay.<sup>45</sup> The membrane preparation was diluted with 4 mL of Dulbecco's phosphate-buffered saline (pH 7.4) and homogenized before use for the stability check. The final protein concentration was 14.9 µg/mL.

Ten microliters of a 2 mg/mL aqueous solution of each nucleotide derivative was mixed with either 90 µL of HCl buffer (pH 1.2) or the membrane suspension and incubated at 37 °C. At regular intervals, a 6 µL aliquot of the above mixture (either membranes or low pH) was removed. The injection sample was prediluted with 54 µL of 5 mM TBAP to allow complete equilibration with the mobile phase to avoid the early HPLC elution at ~1 min. Then, 50 µL of the mixture was injected to the HPLC.

The areas under the curve (AUCs) of compounds were measured using a Hewlett Packard 1100 HPLC equipped with a Zorbax Eclipse 5 mm XDB-C18 analytical column (250 mm  $\times$  4.6 mm; Agilent Technologies Inc., Palo Alto, CA). Mobile phase: linear gradient solvent system: 5 mM TBAP-CH<sub>3</sub>CN from 80:20 to 40:60 in 6.5 min; the flow rate was 1 mL/min (system C) or system B. Peaks were detected by UV absorption with a diode array detector at 254, 275, and 280 nm, and AUCs were calculated based on the peak at 254 nm.

## ■ ASSOCIATED CONTENT

**S Supporting Information.** NMR and mass spectra and HPLC traces for selected derivatives, X-ray structure of N<sup>4</sup>-*t*-BuO-cytosine, and NOESY experiment. This material is available free of charge via the Internet at <http://pubs.acs.org>.

## ■ AUTHOR INFORMATION

### Corresponding Author

\*Tel: 301-496-9024. Fax: 301-480-8422. E-mail: [kajacobs@helix.nih.gov](mailto:kajacobs@helix.nih.gov).

## ■ ACKNOWLEDGMENT

X-ray determination was performed by Dr. Yoshiaki Oyama, Asubio Pharmaceuticals (Osaka, Japan). Mass spectral measurements were performed by Dr. Noel Whittaker (NIDDK). We thank Dr. Francesca Deflorian (NIDDK) and Dr. Andrei A. Ivanov (Emory University) for helpful discussions. This research was supported in part by NIGMS research grant

GM38213 and by the Intramural Research Program of NIDDK, National Institutes of Health. H.M. thanks Asubio Pharma Co., Ltd. for financial support. S.d.C. thanks Ministerio de Educación y Ciencia (Spain) for financial support.

## ABBREVIATIONS USED

CTP, cytidine 5'-triphosphate; DIC, *N,N'*-diisopropylcarbodiimide; DMF, *N,N*-dimethylformamide; EL, extracellular loop; GPCR, G protein-coupled receptor; HEPES, *N*-2-hydroxyethylpiperazine-*N'*-2-ethanesulfonic acid; HPLC, high-performance liquid chromatography; IL, intracellular loop; MOE, molecular operating environment; SAR, structure-activity relationship; TBAP, tetrabutylammonium dihydrogenphosphate; TEAA, triethylammonium acetate; TEMPO, 2,2,6,6-tetramethylpiperidine-1-oxyl; TM, transmembrane  $\alpha$ -helix; TMS, trimethylsilyl; UMP, uridine 5'-monophosphate; UDP, uridine 5'-diphosphate; UTP, uridine 5'-triphosphate

## REFERENCES

- (1) Abbracchio, M. P.; Burnstock, G.; Boeynaems, J. M.; Barnard, E. A.; Boyer, J. L.; Kennedy, C.; Fumagalli, M.; King, B. F.; Gachet, C.; Jacobson, K. A.; Weisman, G. A. International Union of Pharmacology LVIII: Update on the P2Y G protein-coupled nucleotide receptors: From molecular mechanisms and pathophysiology to therapy. *Pharmacol. Rev.* **2006**, *58*, 281–341.
- (2) Brunschweiler, A.; Müller, C. E. P2 Receptors activated by uracil nucleotides—An update. *Curr. Med. Chem.* **2006**, *13*, 289–312.
- (3) Nicholas, R. A.; Lazarowski, E. R.; Watt, W. C.; Li, Q.; Harden, T. K. Uridine nucleotide selectivity of three phospholipase C-activating P2 receptors: Identification of a UDP-selective, a UTP-selective, and an ATP- and UTP-specific receptor. *Mol. Pharmacol.* **1996**, *50*, 224–229.
- (4) Communi, D.; Motte, S.; Boeynaems, J. M.; Piroton, S. Pharmacological characterization of the human P2Y<sub>4</sub> receptor. *Eur. J. Pharmacol.* **1996**, *317*, 383–389.
- (5) Shaver, S. R.; Rideout, J. L.; Pendergast, W.; Douglass, J. G.; Brown, E. G.; Boyer, J. L.; Patel, R. L.; Redick, C. C.; Jones, A. C.; Picher, M.; Yerxa, B. R. Structure activity relationships of dinucleotides: Potent and selective agonists of P2Y receptors. *Purinergic Signalling* **2005**, *1*, 183–191.
- (6) Yerxa, B. R.; Sabater, J. R.; Davis, C. W.; Stutts, M. J.; Lang-Furr, M.; Picher, M.; Jones, A. C.; Cowlen, M.; Dougherty, R.; Boyer, J.; Abraham, W. M.; Boucher, R. C. Pharmacology of INS37217 [P(1)-(uridine 5')-P(4)-(2'-deoxycytidine 5')tetraphosphate, tetrasodium salt], a next-generation P2Y<sub>2</sub> receptor agonist for the treatment of cystic fibrosis. *J. Pharmacol. Exp. Ther.* **2002**, *302*, 871–880.
- (7) Kellerman, D.; Rossi Mospan, A.; Engels, J.; Schaberg, A.; Gorden, A.; Smiley, L. Denufosal: A review of studies with inhaled P2Y<sub>2</sub> agonists that led to Phase 3. *Pulm. Pharmacol. Ther.* **2008**, *21*, 600–607.
- (8) Jacobson, K.; Costanzi, S.; Ivanov, A.; Tchilibon, S.; Besada, P.; Gao, Z.; Maddileti, S.; Harden, T. Structure activity and molecular modeling analyses of ribose- and base-modified uridine 5'-triphosphate analogues at the human P2Y<sub>2</sub> and P2Y<sub>4</sub> receptors. *Biochem. Pharmacol.* **2006**, *71*, 540–549.
- (9) Davenport, R. J.; Diaz, P.; Galvin, F. C.; Lloyd, S.; Mack, S. R.; Owens, R.; Sabin, V.; Wynn, J. Novel nucleotide triphosphates as potent P2Y<sub>2</sub> agonists with enhanced stability over UTP. *Bioorg. Med. Chem. Lett.* **2007**, *17*, 558–561.
- (10) Ivanov, A.; Ko, H.; Cosyn, L.; Maddileti, S.; Besada, P.; Fricks, I.; Costanzi, S.; Harden, T.; Calenbergh, S.; Jacobson, K. Molecular modeling of the human P2Y<sub>2</sub> receptor and design of a selective agonist, 2'-amino-2'-deoxy-2-thiouridine 5'-triphosphate. *J. Med. Chem.* **2007**, *50*, 1166–1176.
- (11) Kim, H. S.; Ravi, R. G.; Marquez, V. E.; Maddileti, S.; Wihlborg, A. -K.; Erlinge, D.; Malmjö, M.; Boyer, J. L.; Harden, T. K.; Jacobson, K. A. Methanocarba modification of uracil and adenine nucleotides: High potency of Northern ring conformation at P2Y<sub>1</sub>, P2Y<sub>2</sub>, P2Y<sub>4</sub> and P2Y<sub>11</sub>, but not P2Y<sub>6</sub> receptors. *J. Med. Chem.* **2002**, *45*, 208–218.
- (12) El-Tayeb, A.; Qi, A.; Müller, C. E. Synthesis and Structure-Activity Relationships of Uracil Nucleotide Derivatives and Analogues as Agonists at Human P2Y<sub>2</sub>, P2Y<sub>4</sub>, and P2Y<sub>6</sub> Receptors. *J. Med. Chem.* **2006**, *49*, 7076–7087.
- (13) Ko, H.; Carter, R. L.; Cosyn, L.; Petrelli, R.; de Castro, S.; Besada, P.; Zhou, Y.; Cappellacci, L.; Franchetti, P.; Grifantini, M.; Van Calenbergh, S.; Harden, T. K.; Jacobson, K. A. Synthesis and potency of novel uracil nucleotide analogues as P2Y<sub>2</sub> and P2Y<sub>6</sub> receptor agonists. *Bioorg. Med. Chem.* **2008**, *16*, 6319–6332.
- (14) Sauer, R.; El-Tayeb, A.; Kaulich, M.; Müller, C. E. Synthesis of uracil nucleotide analogs with a modified, acyclic ribose moiety as P2Y<sub>2</sub> receptor antagonists. *Bioorg. Med. Chem.* **2009**, *17*, 5071–5079.
- (15) Maruoka, H.; Barrett, M. O.; Ko, H.; Tosh, D. K.; Melman, A.; Burianek, L. E.; Balasubramanian, R.; Berk, B.; Costanzi, S.; Harden, T. K.; Jacobson, K. A. Pyrimidine Ribonucleotides with Enhanced Selectivity as P2Y<sub>6</sub> Receptor Agonists: Novel 4-Alkylxyimino, (S)-Methanocarba, and 5'-Triphosphate  $\gamma$ -Ester Modifications. *J. Med. Chem.* **2010**, *53*, 4488–4501.
- (16) Wu, B.; Chien, E. Y.; Mol, C. D.; Fenalti, G.; Liu, W.; Katritch, V.; Abagyan, R.; Brooun, A.; Wells, P.; Bi, F. C.; Hamel, D. J.; Kuhn, P.; Handel, T. M.; Cherezov, V.; Stevens, R. C. Structures of the CXCR4 chemokine GPCR with small-molecule and cyclic peptide antagonists. *Science* **2010**, *330*, 1066–1071.
- (17) Kogo, S.; Yamada, K.; Iwai, Y.; Osawa, K.; Hayakawa, H. Process for Producing Di(pyrimidine nucleoside 5'-)polyphosphate. WO2008/012949 A1, 2008.
- (18) Heeres, A.; van Doren, H. A.; Gotlieb, K. F.; Bleeker, I. P. Synthesis of  $\alpha$ - and  $\beta$ -D-glucopyranuronate 1-phosphate and  $\alpha$ -D-glucopyranuronate 1-fluoride: Intermediates in the synthesis of D-glucuronic acid from starch. *Carbohydr. Res.* **1997**, *299*, 221–227.
- (19) Bourdon, D. M.; Wing, M. R.; Edwards, E. B.; Sondek, J.; Harden, T. K. Quantification of isozyme-specific activation of phospholipase C- $\beta$  2 by Rac GTPases and phospholipase C- $\epsilon$  by Rho GTPases in an intact cell assay system. *Methods Enzymol.* **2006**, *406*, 489–499.
- (20) Costanzi, S.; Mamedova, L.; Gao, Z.; Jacobson, K. Architecture of P2Y nucleotide receptors: structural comparison based on sequence analysis, mutagenesis, and homology modeling. *J. Med. Chem.* **2004**, *47*, 5393–5404.
- (21) de Castro, S.; Maruoka, H.; Hong, K.; Kilbey, S. M., 2nd; Costanzi, S.; Hechler, B.; Brown, G. G., Jr; Gachet, C.; Harden, T. K.; Jacobson, K. A. Functionalized congeners of P2Y<sub>1</sub> receptor antagonists: 2-alkynyl (N)-methanocarba 2'-deoxyadenosine 3',5'-bisphosphate analogues and conjugation to a polyamidoamine (PAMAM) dendrimer carrier. *Bioconjugate Chem.* **2010**, *21*, 1190–205.
- (22) Hoffmann, C.; Moro, S.; Nicholas, R. A.; Harden, T. K.; Jacobson, K. A. The role of amino acids in extracellular loops of the human P2Y<sub>1</sub> receptor in surface expression and activation processes. *J. Biol. Chem.* **1999**, *274*, 14639–14647.
- (23) Moro, S.; Hoffmann, C.; Jacobson, K. A. Role of the extracellular loops of G protein-coupled receptors in ligand recognition: a molecular modeling study of the human P2Y<sub>1</sub> receptor. *Biochemistry* **1999**, *38*, 3498–3507.
- (24) Hillmann, P.; Ko, G. Y.; Spinrath, A.; Raulf, A.; von Kugelgen, I.; Wolff, S. C.; Nicholas, R. A.; Kostenis, E.; Holtje, H. D.; Müller, C. E. Key determinants of nucleotide-activated G protein-coupled P2Y<sub>2</sub> receptor function revealed by chemical and pharmacological experiments, mutagenesis and homology modeling. *J. Med. Chem.* **2009**, *52*, 2762–2775.
- (25) Moro, S.; Guo, D.; Camaioni, E.; Boyer, J. L.; Harden, T. K.; Jacobson, K. A. Human P2Y<sub>1</sub> receptor: molecular modeling and site-directed mutagenesis as tools to identify agonist and antagonist recognition sites. *J. Med. Chem.* **1998**, *41*, 1456–66.

(26) Jiang, Q.; Guo, D.; Lee, B. X.; van Rhee, A. M.; Kim, Y. C.; Nicholas, R. A.; Schachter, J. B.; Harden, T. K.; Jacobson, K. A. A mutational analysis of residues essential for ligand recognition at the human P2Y<sub>1</sub> receptor. *Mol. Pharmacol.* **1997**, *52*, 499–507.

(27) Van Meervelt, L. Structure of 3',5'-di-O-acetyl-N<sup>4</sup>-methoxycytosine. *Acta Crystallogr.* **1991**, *C47*, 2635–2637.

(28) Ballesteros, J. A.; Weinstein, H. Integrated methods for the construction of three-dimensional models and computational probing of structure-function relations in G protein-coupled receptors. In *Methods in Neurosciences*; Stuart, C. S., Ed.; Academic Press: San Diego, 1995; Vol. 25, pp 366–428.

(29) van Rhee, A. M.; Jacobson, K. A. Molecular architecture of G protein-coupled receptors. *Drug Dev. Res.* **1996**, *37*, 1–38.

(30) Costanzi, S.; Tikhonova, I.; Ohno, M.; Roh, E.; Joshi, B.; Colson, A.; Houston, D.; Maddileti, S.; Harden, T.; Jacobson, K. P2Y<sub>1</sub> antagonists: Combining receptor-based modeling and QSAR for a quantitative prediction of the biological activity based on consensus scoring. *J. Med. Chem.* **2007**, *50*, 3229–3241.

(31) Yitzhaki, S.; Shneyvays, V.; Jacobson, K. A.; Shainberg, A. Involvement of uracil nucleotides in protection of cardiomyocytes from hypoxic stress. *Biochem. Pharmacol.* **2005**, *69*, 1215–1223.

(32) Wildman, S. S.; Unwin, R. J.; King, B. F. Extended pharmacological profiles of rat P2Y<sub>2</sub> and rat P2Y<sub>4</sub> receptors and their sensitivity to extracellular H<sup>+</sup> and Zn<sup>2+</sup> ions. *Br. J. Pharmacol.* **2003**, *140*, 1177–1186.

(33) Robaye, B.; Ghanem, E.; Wilkin, F.; Fokan, D.; Van Driessche, W.; Schurmans, S.; Boeynaems, J. M.; Beauwens, R. Loss of nucleotide regulation of epithelial chloride transport in the jejunum of P2Y<sub>4</sub>-null mice. *Mol. Pharmacol.* **2003**, *63*, 777–783.

(34) Ghanem, E.; Robaye, B.; Leal, T.; Leipziger, J.; Van Driessche, W.; Beauwens, R.; Boeynaems, J. M. The role of epithelial P2Y<sub>2</sub> and P2Y<sub>4</sub> receptors in the regulation of intestinal chloride secretion. *Br. J. Pharmacol.* **2005**, *146*, 364–369.

(35) Matos, J. E.; Sorensen, M. V.; Geyti, C. S.; Robaye, B.; Boeynaems, J. M.; Leipziger, J. Distal colonic Na<sup>+</sup> absorption inhibited by luminal P2Y<sub>2</sub> receptors. *Pflugers Arch.* **2007**, *454*, 977–987.

(36) Cosentino, S.; Barcella, S.; Lo, H.; Burbiel, J. C.; Müller, C. E.; Tremoli, E.; Banfi, C.; Abbracchio, M. P. Role of P2 receptors in a cardiomyocyte ischemic hypoxia model. Purines2010, Tarragona, Spain. May 30–June 2, 2010. Abstract P10–11.

(37) Horckmans, M.; Lantz, N.; Dol-Gleizes, F.; Savi, P.; Gachet, C.; Boeynaems, J. M.; Robaye, B.; Communi, D. Involvement of the P2Y<sub>4</sub> receptor in inflammation and angiogenesis. Purines 2008 Meeting June 29–July 2, 2008, Copenhagen, Denmark. *Purinergic Signalling* **2008**, *4* (Suppl. 1), 118.

(38) Vanderstocken, G.; Bondue, B.; Horckmans, M.; Di Pietrantonio, L.; Robaye, B.; Boeynaems, J. M.; Communi, D. P2Y<sub>2</sub> receptor regulates VCAM-1 membrane and soluble forms and eosinophil accumulation during lung inflammation. *J. Immunol.* **2010**, *185*, 3702–3707.

(39) MacDonald, D. L. [11] Chemical synthesis of aldose 1-phosphates. *Methods Enzymol.* **1966**, *8*, 121–125.

(40) *The Molecular Operating Environment (MOE)*; Chemical Computing Group, Inc.: Montreal, Canada, 2009; Vol. 10; www.ccg.com.

(41) Labute, P. The generalized Born/volume integral implicit solvent model: Estimation of the free energy of hydration using London dispersion instead of atomic surface area. *J. Comput. Chem.* **2008**, *29*, 1693–1698.

(42) *Maestro*, 9.1; Schrodinger, LLC: New York, NY; www.schrodinger.com.

(43) *MacroModel*, 9.8; Schrodinger, LLC: New York, NY; www.schrodinger.com.

(44) *SiteMap*, 2.4; Schrödinger, LLC: New York, NY; www.schrodinger.com.

(45) Bradford, M. M. A rapid and sensitive method for the quantitation of microgram quantities of protein utilizing the principle of protein dye binding. *Anal. Biochem.* **1976**, *76*, 248–254.